Truncated Modified Weighted Exponential Distribution with Different Estimation Methods and Applications

Amer Ibrahim Al-Omari[1,*], Khaoula Aidi[2] and Ghadah Alomani[3]

[1] Department of Mathematics, Faculty of Science, Al Al-Bayt University, Mafraq, 25113, Jordan

[2] Laboratory of Probability and Statistics LaPS, Badji Mokhtar-Annaba University, P.O. Box 12, Annaba, 23000, Algeria

[3] Department of Mathematical Sciences, College of Science, Princess Nourah bint Abdulrahman University, P.O. Box 84428, Riyadh, 11671, Saudi Arabia

INFORMATION

Keywords:
Truncated distribution
modified weighted exponential distribution
maximum likelihood estimation
distribution theory
weighted least squares
Anderson-Darling estimation

DOI: 10.23967/j.rimni.2025.10.71900

SCIPEDIA Revista Internacional de Métodos Numéricos para Cálculo y Diseño en Ingeniería

Revista Internacional Métodos numéricos para cálculo y diseño en ingeniería RIMNI in cooperation with CIMNE

Truncated Modified Weighted Exponential Distribution with Different Estimation Methods and Applications

Amer Ibrahim Al-Omari[1,*], Khaoula Aidi[2] and Ghadah Alomani[3]

[1]Department of Mathematics, Faculty of Science, Al Al-Bayt University, Mafraq, 25113, Jordan

[2]Laboratory of Probability and Statistics LaPS, Badji Mokhtar-Annaba University, P.O. Box 12, Annaba, 23000, Algeria

[3]Department of Mathematical Sciences, College of Science, Princess Nourah bint Abdulrahman University, P.O. Box 84428, Riyadh, 11671, Saudi Arabia

ABSTRACT

This study introduces the Truncated Modified Weighted Exponential (TrMWE) Distribution, developed by extending the traditional modified weighted exponential distribution with an additional parameter and truncating its support to a finite range, enhancing its adaptability for modeling lifetime and reliability data. The statistical properties of the TrMWE, including moments, the moment-generating function, the quantile function, and order statistics, are examined. Parameter estimation is performed via maximum likelihood estimation (MLE), least squares and weighted least squares methods, maximum product of spacing method, Cramer-Von-Mises method, Anderson-Darling method, and right and left tails Anderson-Darling methods, with analysis of the asymptotic behavior of the estimators. Rényi and Tsallis entropies are also derived to assess the distribution's uncertainty. The practicality of the TrMWE is illustrated using three real datasets and compared with existing distributions based on goodness-of-fit criteria, such as the Akaike Information Criterion and Bayesian Information Criterion. The results highlight the distribution's flexibility and superior performance in modeling complex datasets.

OPEN ACCESS

Received: 14/08/2025

Accepted: 05/11/2025

Published: 03/02/2026

DOI
10.23967/j.rimni.2025.10.71900

Keywords:
Truncated distribution
modified weighted exponential distribution
maximum likelihood estimation
distribution theory
weighted least squares
Anderson-Darling estimation

1 Introduction

The development of proposed probability density function (PDF) plays a vital role in statistical analysis and modeling, especially when existing distributions fall short in accurately reflecting the patterns present in real-world data. Such a PDF typically introduces greater flexibility, enabling improved modeling of features like skewness, peakedness, and tail behavior in complex datasets. This added adaptability is particularly beneficial in domains such as reliability studies, survival analysis, and risk modeling, where precise data representation is essential for sound decision-making. Additionally, proposing a new PDF often contributes to the advancement of statistical theory and provides valuable

*Correspondence: Amer Ibrahim Al-Omari (alomari_amer@yahoo.com).

tools for tasks like parameter estimation, goodness-of-fit evaluation, and model selection, thereby enriching the array of techniques available to analysts and researchers.

Let X be a random variable with probability density function (PDF) $f(x;\Omega)$ and cumulative distribution function (CDF) $F(x;\Omega)$. A distribution $G(x,\Omega)$ is said to be a double truncated distribution over the interval $[\phi,\varphi]$ if its CDF is given by:

$$G(x;\Omega)=\frac{F(x;\Omega)-F(\phi;\Omega)}{F(\varphi;\Omega)-F(\phi;\Omega)}, \tag{1}$$

where $(\phi\le x\le\varphi)$ and $-\infty<\phi<\varphi<\infty$, with PDF defined as:

$$g(x;\Omega)=\frac{f(x;\Omega)}{F(\varphi;\Omega)-F(\phi;\Omega)},\quad \phi\le x\le\varphi. \tag{2}$$

Here, there are three cases: (1) If $\phi=0$ and $\varphi\to\infty$, it reduces to the baseline model. (2) When $\phi=0$, it is an upper truncated distribution. (3) As $\varphi\to\infty$, it is a lower truncated distribution. Zaninetti [1] proposed right and left truncated gamma distribution. Singh et al. [2] proposed truncated Lindley distribution. Aguilar et al. [3] proposed zero-truncated Poisson exponentiated gamma distribution. Shukla et al. [4] proposed zero-truncated Poisson-Ishita distribution. Dey et al. [5] considered the reflected-shifted-truncated Lomax distribution. Alotaibi et al. [6] suggested truncated Cauchy power Weibull-G class of distributions. Badr et al. [7] proposed the zero truncated Poisson-Pareto distribution, derived by compounding the Pareto and zero-truncated Poisson distributions, provides enhanced flexibility for modeling real datasets. Abbas et al. [8] suggested truncated Weibull-exponential distribution. Hussein et al. [9] suggested a new truncated Lindley-generated family of distributions with regression analysis. Teamah and Elmenify [10] considered doubly truncated generalized log-Lindley distribution. Eledum and El-Alosey [11] proposed discrete Kumaraswamy Erlang-truncated exponential distribution.

Sen et al. [12] investigated truncated versions of the Xgamma distribution, Xgamma distribution, Zinodiny et al. [13] offered truncated matrix variate gamma distribution. Liu et al. [14] considered evaluation of wind energy using a truncated distribution approach for probabilistic turbulence power spectral parameters. Various the literature about truncated family of distributions are suggested as truncated Fréchet generated (TF-G) family by Abid and Abdulrazak [15], truncated inverted Kumaraswamy generated family introduced by Bantan et al. [16], and transmuted Muth generated (TM-G) family proposed by Al-Babtain et al. [17]. For a continuous distribution with support $(0,\infty)$ with CDF $F(x,\Omega)$ a new truncation method is defined by Nik et al. [18] as

$$F_*(x,\Omega)=\frac{F(x,\Omega)}{F_*(b,\Omega)}, x\in(0,b),$$

where $F_*(x,\Omega)=1$ if $x\ge b$, and $F_*(x,\Omega)=0$ if $x\le 0$. Also, they defined another form of truncated distributions given by:

$$F_{**}(x,\Omega)=F\left(\frac{bx}{b-x}\right), x\in(0,b),$$

where $F_{**}(x,\Omega)=1$ if $x\ge b$, and $F_{**}(x,\Omega)=0$ if $x\le 0$.

Recently, reference [19] introduced the modified weighted exponential distribution (MWED) with PDF and CDF, respectively are given by:

$$f(x,\alpha,\lambda) = \lambda e^{-\lambda x}\left(\frac{\alpha+2}{\alpha+1} - e^{-\alpha\lambda x}\right), x > 0, \alpha \geq 0, \lambda > 0, \tag{3}$$

and

$$F(x,\alpha,\lambda) = 1 - \frac{e^{-\lambda x}(\alpha+2-e^{-\alpha\lambda x})}{\alpha+1}. \tag{4}$$

Fig. 1 shows the PDF plots of the MWED for $\alpha = 0.6, 6$ and $\lambda = 0.2, 1, 9$. It can be seen that the distribution has many shapes include decreasing and increasing-decreasing.

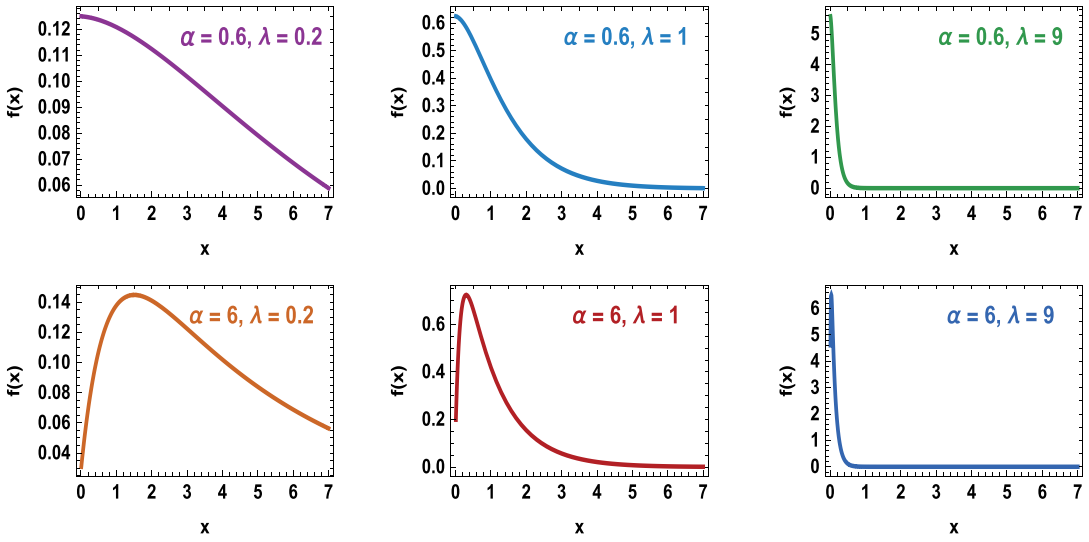

Figure 1: The pdf plots of the MWED for $\alpha = 0.6, 6$ and $\lambda = 0.2, 1, 9$

The MWED is a two-parameter offers a simple yet flexible lifetime model by mixing exponential and weighted exponential distributions without adding extra parameters. It supports decreasing or unimodal PDFs and ensures an increasing hazard rate function. Finally, simulation studies and applications to real data confirm that it performs competitively against established models like Weibull, gamma, and generalized exponential, highlighting its practical relevance across applied domains.

The remainder of the paper is organized as follows. Section 2 introduces the proposed TrMWED distribution, detailing its definition and key properties. Section 3 presents its statistical characteristics, including reliability functions, moments, the quantile function, Tsallis and Rényi entropies, order statistics, the mean residual life function, mean inactivity time, and the vitality function. Section 4 addresses parameter estimation using maximum likelihood, least squares and weighted least squares, the maximum product of spacings, and goodness-of-fit–based methods such as the Cramér-von Mises, Anderson-Darling, and right- and left-tail Anderson-Darling tests. A Monte Carlo simulation study is conducted in Section 5. Section 6 demonstrates the application of the TrMWED distribution to three real-life datasets and compares its performance with some existing models using various goodness-of-fit criteria. Finally, Section 7 concludes with a summary of key findings and suggestions for future research.

2 The Proposed Distribution

Here, we will consider the upper truncated case with the base distribution given in Eq. (3) to suggest the TrMWE distribution on the support $(0, b)$ with PDF given by:

$$g(x;\alpha,\lambda,b) = \frac{(\alpha+1)\lambda e^{-\lambda x}\left(\frac{\alpha+2}{\alpha+1} - e^{-\alpha\lambda x}\right)}{1+\alpha+e^{-(\alpha+1)b\lambda} - (\alpha+2)e^{-b\lambda}}$$
$$= \frac{1}{\psi}\left((\alpha+1)\lambda e^{-\lambda x}\left(\frac{\alpha+2}{\alpha+1} - e^{-\alpha\lambda x}\right)\right), \quad 0 < x \le b, \alpha \ge 0, \lambda > 0, \tag{5}$$

$\psi = 1+\alpha+e^{-(\alpha+1)b\lambda} - (\alpha+2)e^{-b\lambda}$. To find the mode of the distribution, since the ψ is a positive normalizing constant, the mode depends only on the numerator:

$$h(x) = (\alpha+1)\lambda e^{-\lambda x}\left(\frac{\alpha+2}{\alpha+1} - e^{-\alpha\lambda x}\right).$$

Differentiate $h(x)$ with respect to x as:

$$h'(x) = -(\alpha+1)\lambda^2 e^{-\lambda x}\left(\frac{\alpha+2}{\alpha+1} - e^{-\alpha\lambda x}\right) + (\alpha+1)\lambda e^{-\lambda x}\cdot(\alpha\lambda)e^{-\alpha\lambda x}.$$

Set $h'(x) = 0$, then solve to x to get:

$$x^* = \frac{1}{\alpha\lambda}\ln\left(\frac{(\alpha+1)^2}{\alpha+2}\right), \quad \alpha > 0,$$

and hence the mode of the distribution is given by:

$$x_{\text{mode}} = \begin{cases} 0, & 0 \le \alpha < \frac{\sqrt{5}-1}{2}, \\ \min\{x^*, b\}, & \alpha \ge \frac{\sqrt{5}-1}{2}. \end{cases}$$

Fig. 2 explains the PDf plots of the TrMWED for $b = 1, 8$ with $(\alpha,\lambda) = (0.1, 0.2), (0.2, 0.3), (0.3, 0.4), (0.4, 0.5), (0.5, 0.6), (0.6, 0.7)$ and for $b = 1, 4$ with $(\alpha,\lambda) = (1, 2), (2, 3), (3, 4), (4, 5), (5, 6), (0.6, 0.7)$. It is clear that the TrMWED PDF curve is decreasing and increasing-decreasing making the distribution more flexible in fitting various data.

The CDF of the suggested TrMWED is given by:

$$G(x,\alpha,\lambda,b) = \frac{1}{\psi}\left(1+\alpha+e^{-(\alpha+1)\lambda x} - (\alpha+2)e^{-\lambda x}\right), \tag{6}$$

where $\psi = 1+\alpha+e^{-(\alpha+1)b\lambda} - (\alpha+2)e^{-b\lambda}$.

3 Properties of the TrMWED

This section presents the main statistical properties of the distribution, including reliability functions, moments, the quantile function, Tsallis and ényi entropies, order statistics, the mean residual life function, mean inactivity time, and the vitality function.

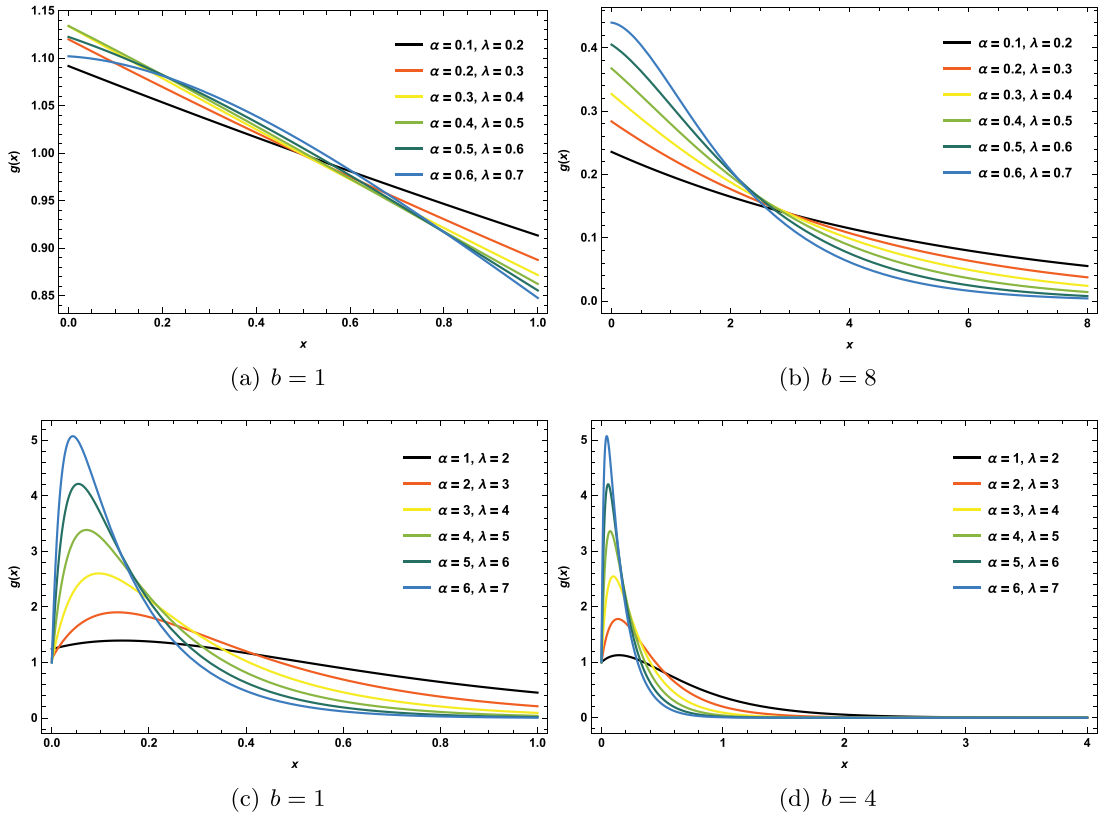

(a) $b = 1$ (b) $b = 8$

(c) $b = 1$ (d) $b = 4$

Figure 2: PDF plots of the TrMWED for some selected parameters

3.1 Reliability Functions

The survival function, $S(x)$, expresses the probability that a random variable X, which often represents a lifespan or time until an event occurs, is greater than a specified value x. Mathematically, it is given by:

$$S(x) = P(X > x) = 1 - G(x).$$

For the TrMWED it is defined as:

$$S(x, \alpha, \lambda, b) = 1 - \frac{1}{\psi}\left(1 + \alpha + e^{-(\alpha+1)\lambda x} - (\alpha + 2)e^{-\lambda x}\right), \tag{7}$$

where $\psi = 1 + \alpha + e^{-(\alpha+1)b\lambda} - (\alpha + 2)e^{-b\lambda}$. In Fig. 3, the survival function plots of the TrMWED for $b = 1$ with some values of λ and α are provided.

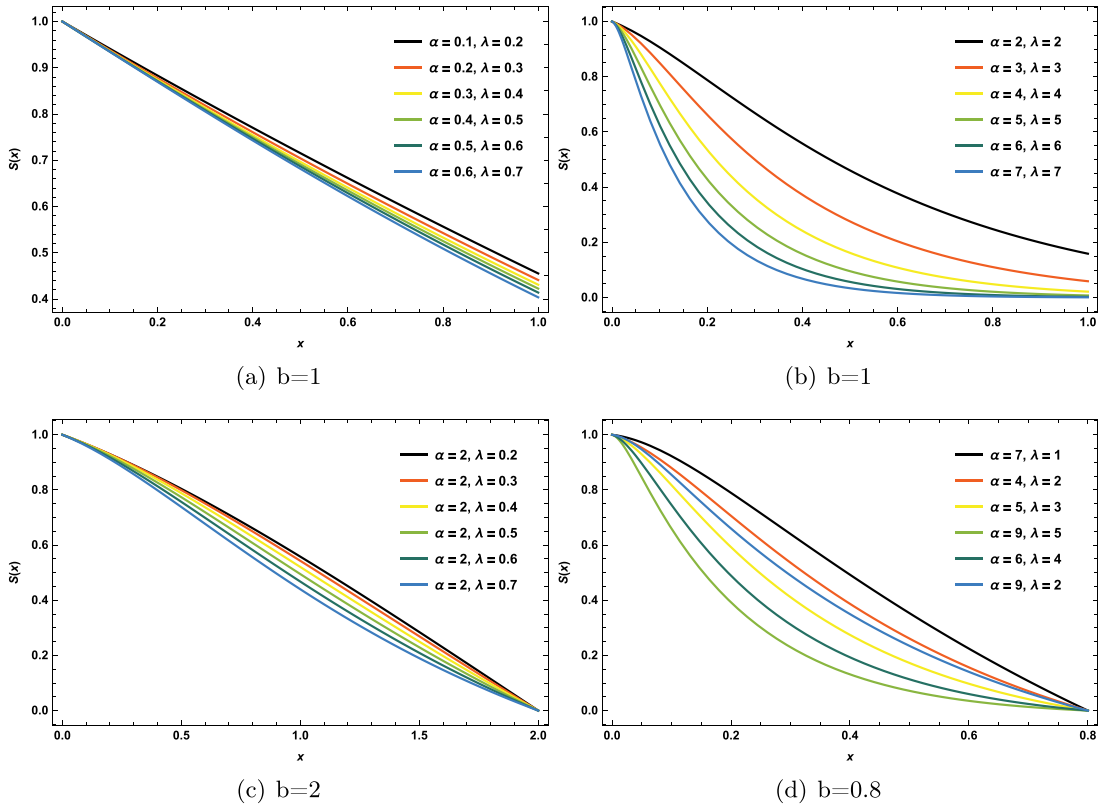

(a) b=1 (b) b=1

(c) b=2 (d) b=0.8

Figure 3: Survival function plots of the TrMWED for some values of b, λ, and α

The hazard rate function (HrF) is one of the most important properties for justifying model selection. For the TrMWED, the HrF is given by:

$$HrF(x,\alpha,\lambda,b) = \frac{\lambda\left((\alpha+2)e^{\alpha\lambda x} - \alpha - 1\right)e^{\lambda[(\alpha+2)b+x]}}{(\alpha+2)\left[e^{\lambda[\alpha(b+x)+2b+x]} - e^{\lambda[\alpha(b+x)+b+2x]}\right] - e^{\lambda[(\alpha+2)b+x]} + e^{\lambda[b+(\alpha+2)x]}}.$$

Fig. 4 shows the hazard rate function plots of the TrMWED for $b = 9$, $\alpha = 2, 3$ and $\lambda = 0.2, 0.8, 1, 2, 5, 8$. Also, for $b = 1$, $\alpha = 3, 5, 9$ and $\lambda = 3$.

The hazard rate function $HrF(x,\alpha,\lambda,b)$ at $x = 0$ is finite and positive, where $HrF(0,\alpha,\lambda,b) = \frac{\lambda e^{\lambda(\alpha+2)b}}{(\alpha+1)e^{\lambda(\alpha+2)b} - (\alpha+2)e^{\lambda(\alpha+1)b} + e^{\lambda b}}$. Also, for $\alpha = 1$, $\lambda = 1$, $b = 1$, at $x = 0$, we have $HrF(0) \approx 0.969$. It is infinite at $x = b$, since the denominator becomes zero while the numerator remains positive, so $HrF(b,\alpha,\lambda,b) \to \infty$. However, it is increasing over $0 < x \leq b$ because for $\alpha = 0$, the hazard rate simplifies to $HrF(x,0,\lambda,b) = \frac{\lambda e^{\lambda(2b+x)}}{e^{\lambda(2b+x)} - e^{\lambda(b+2x)}}$, with derivative $\frac{d}{dx}HrF(x) = \frac{\lambda^2 e^{\lambda(2b+x)}e^{\lambda(b+2x)}}{\left(e^{\lambda(2b+x)} - e^{\lambda(b+2x)}\right)^2} > 0$, confirming monotonicity. Finally, the exponential growth in the numerator and decreasing denominator support an increasing trend.

The reversed hazard rate function (RHrF) of the TrMWED is defined as:

$$RHrF(x,\alpha,\lambda,b) = \frac{(\alpha+1)\lambda e^{-\lambda x}\left(\frac{\alpha+2}{\alpha+1} - e^{-\alpha\lambda x}\right)}{1+\alpha+e^{-(\alpha+1)\lambda x} - (\alpha+2)e^{-\lambda x}}.$$

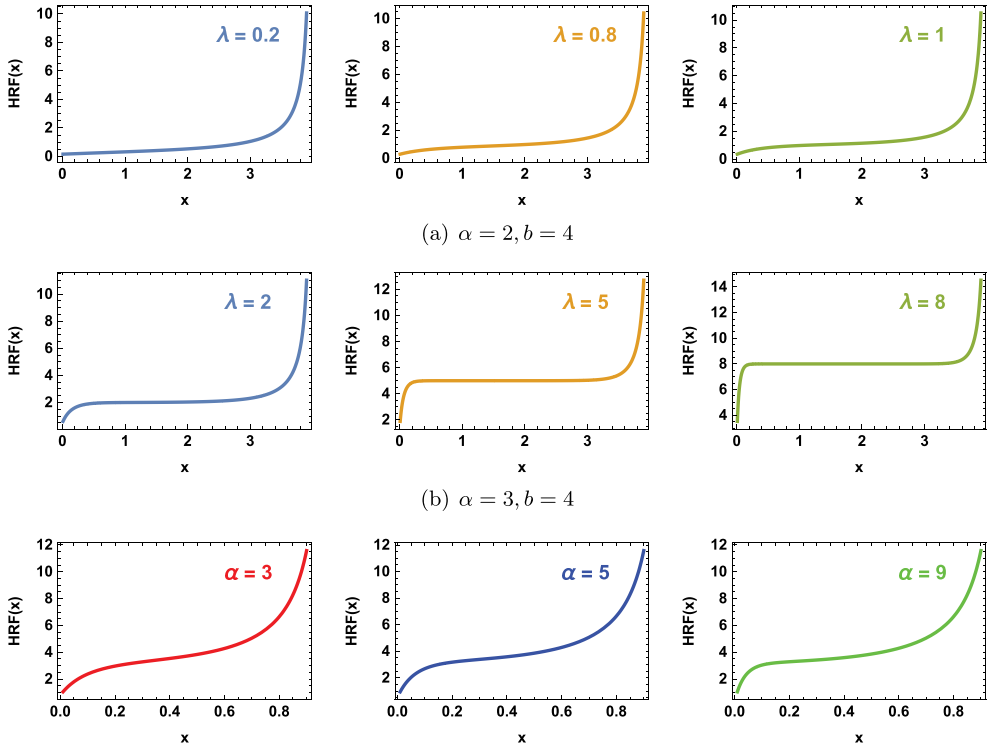

(a) $\alpha = 2, b = 4$

(b) $\alpha = 3, b = 4$

(c) $\lambda = 3, b = 1$

Figure 4: Hazard rate function plots of the TrMWED for $\lambda = 0.2, 0.8, 1, 2, 5, 8, \alpha = 2, 3, 5$, and $b = 1, 4$

Fig. 5 displays the reversed hazard rate function plots of the TrMWED for $b = 9$, $\alpha = 0.6$ and $\lambda = 0.2, 0.8, 1, 5, 7, 9$.

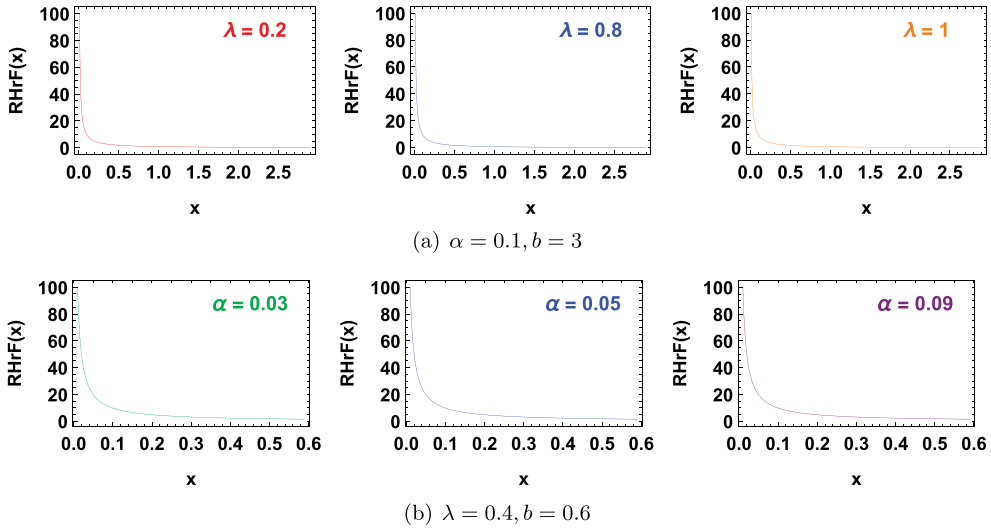

(a) $\alpha = 0.1, b = 3$

(b) $\lambda = 0.4, b = 0.6$

Figure 5: The TrMWED RHrF(x) plots for $b = 0.6, 3$, $\alpha = 0.03, 0.05, 0.09, 0.1$ and $\lambda = 0.2, 0.4, 0.8, 1$

3.2 Quantile Function and Moments

Let X denotes a random variable with the PDF (Eq. (5)). The quantile function, say $Q(p)$, defined by $G[Q(p)] = p$, is the root of the equation:

$$\frac{1}{1+\alpha+e^{-(\alpha+1)b\lambda}-(\alpha+2)e^{-b\lambda}}\left(1+\alpha+e^{-(\alpha+1)\lambda Q(p)}-(\alpha+2)e^{-\lambda Q(p)}\right)=p.$$

Then, the quantile function of the TrMWED is given by:

$$Q(p)=\frac{1}{\lambda}W\left(\frac{p\left(1+e^{-b(1+\alpha)\lambda}+\alpha-e^{-b\lambda}(2+\alpha)\right)-(1+\alpha)}{2+\alpha}\right), \tag{8}$$

where $W(x)$ is the Lambert function.

The cth moment of the TrMWED is given by:

$$E\left(X^c\right)=\frac{1}{\psi\lambda^c}\left((\alpha+2)\left[\Gamma(c+1)-\Gamma(c+1,b\lambda)\right]+\frac{\Gamma(c+1,b(\alpha+1)\lambda)-c\Gamma(c)}{(\alpha+1)^c}\right), \tag{9}$$

where $\psi=1+\alpha+e^{-(\alpha+1)b\lambda}-(\alpha+2)e^{-b\lambda}$, and $c=1,2,3,\ldots$ Hence, the mean and the second moment, respectively are:

$$E(X)=\frac{1+\alpha(\alpha+3)-(\alpha+1)(\alpha+2)\Gamma(2,b\lambda)+\Gamma\left[2,b(\alpha+1)\lambda\right]}{(\alpha+1)\lambda\psi},$$

and

$$E\left(X^2\right)=\frac{1}{\lambda^2\psi}\left(\frac{\Gamma(3,b(\alpha+1)\lambda)-2}{(\alpha+1)^2}-(\alpha+2)(\Gamma(3,b\lambda)-2)\right).$$

The moment generating function is given by:

$$M_X(t)=\frac{(\alpha+1)\lambda\left(e^{-(\alpha+1)b\lambda}e^{bt}\left(\frac{1}{\alpha\lambda-t+\lambda}-\frac{(\alpha+2)e^{\alpha b\lambda}}{(\alpha+1)(\lambda-t)}\right)+\frac{1}{t-(\alpha+1)\lambda}+\frac{\alpha+2}{(\alpha+1)(\lambda-t)}\right)}{\alpha+e^{-(\alpha+1)b\lambda}-(\alpha+2)e^{-b\lambda}+1},$$

$$\psi=1+\alpha+e^{-(\alpha+1)b\lambda}-(\alpha+2)e^{-b\lambda}.$$

3.3 Entropy Measures

For a continuous random variable X with a PDF $f(x)$, Shannon entropy is defined as:

$$H_1(X)=-\int_{-\infty}^{\infty}f(x)\log f(x)dx.$$

The Rényi entropy Rényi [20] is a generalization of the Shannon entropy that introduces a parameter η to control the weight given to different probabilities, and it is defined as:

$$H_\eta(X)=\frac{1}{1-\eta}\log\left(\int_{-\infty}^{\infty}[f(x)]^\eta\,dx\right),\eta>0,\eta\neq1.$$

For the TrMWED the Rényi entropy is given by:

$$H_\eta(X)=\frac{1}{1-\eta}\log\left(\left(\frac{\alpha+1}{\psi}\right)^\eta\sum_{i=0}^{\eta}\frac{(-1)^i\lambda^{\eta-1}}{\eta+\alpha i}\binom{\eta}{i}\left(\frac{\alpha+2}{\alpha+1}\right)^{\eta-i}\left[1-e^{-b\lambda(\eta+\alpha i)}\right]\right), \tag{10}$$

where $\eta > 0, \eta \neq 1$, and $\psi = 1 + \alpha + e^{-(\alpha+1)b\lambda} - (\alpha + 2)e^{-b\lambda}$.

Tsallis [21] generalized Shanon's entropy to suggest the Tsallis Entropy and defined this measure as:

$$H_{\varrho}(X) = \frac{1}{\varrho - 1}\left(1 - \int_{-\infty}^{\infty} f^{\varrho}(x)dx\right), \varrho > 0, \varrho \neq 1,$$

which for the TrMWED is defined as:

$$H_{\varrho}(X) = \frac{1}{\varrho - 1}\left(1 - \left(\frac{\alpha + 1}{\psi}\right)^{\varrho} \sum_{i=0}^{\varrho} \frac{(-1)^i \lambda^{\varrho-1}}{\varrho + \alpha i}\binom{\varrho}{i}\left(\frac{\alpha + 2}{\alpha + 1}\right)^{\varrho-i}\left[1 - e^{-b\lambda(\varrho+\alpha i)}\right]\right), \tag{11}$$

provided that , $\varrho > 0, \varrho \neq 1$, and $\psi = 1 + \alpha + e^{-(\alpha+1)b\lambda} - (\alpha + 2)e^{-b\lambda}$.

To investigate the behavior of Rényi and Tsallis entropies, numerical values are obtained for both measures and the results are given in Tables 1 and 2, respectively.

Table 1: Numerical values for $H_{\eta}(X)$ for various values of the distribution parameters

	$\lambda = 0.6\ \eta = 3$	$\lambda = 0.6\ \eta = 3$		$\lambda = 0.6\ \alpha = 3$	$\lambda = 0.6\ \alpha = 0.5$
α	$b = 6$	$b = 8$	η	$b = 8$	$b = 8$
2.000	1.302	1.341	2	1.359	1.429
2.300	1.288	1.326	3	1.254	1.321
2.600	1.273	1.311	4	1.192	1.255
2.900	1.260	1.297	5	1.151	1.210
3.200	1.248	1.284	6	1.121	1.177
3.500	1.236	1.272	7	1.098	1.151
3.800	1.226	1.261	8	1.080	1.130
4.100	1.216	1.251	9	1.065	1.113
4.400	1.207	1.242	10	1.053	1.099
4.700	1.199	1.233	11	1.043	1.087
5.000	1.192	1.226	12	1.034	1.077
5.300	1.185	1.218	13	1.026	1.068
5.600	1.178	1.212	14	1.019	1.059

Table 2: Numerical values for $H_{\varrho}(X)$ for various values of the distribution parameters

ϱ	$\lambda = 0.6\ \alpha = 0.5, b = 8$	$\lambda = 0.5\ \alpha = 0.4, b = 4$	$\lambda = 0.8\ \alpha = 2, b = 3$	$\lambda = 0.5\ \alpha = 2, b = 6$
2	0.760	0.710	0.605	0.778
3	0.464	0.454	0.414	0.472
4	0.326	0.323	0.307	0.328
5	0.248	0.247	0.240	0.249
6	0.199	0.199	0.196	0.200
7	0.167	0.166	0.165	0.167

(Continued)

Table 2 (continued)

ϱ	$\lambda = 0.6\ \alpha = 0.5, b = 8$	$\lambda = 0.5\ \alpha = 0.4, b = 4$	$\lambda = 0.8\ \alpha = 2, b = 3$	$\lambda = 0.5\ \alpha = 2, b = 6$
8	0.143	0.143	0.142	0.143
9	0.125	0.125	0.125	0.125
10	0.111	0.111	0.111	0.111
11	0.100	0.100	0.100	0.100
12	0.091	0.091	0.091	0.091
13	0.083	0.083	0.083	0.083
14	0.077	0.077	0.077	0.077

Based on Tables 1 and 2, the Rényi entropy values decrease as α increases for fixed values of b, λ, and η, and also decrease as η increases for fixed values of b, λ, α. Similarly, the Tsallis entropy values decrease for all values of b, λ, α as ρ increases. However, for ρ between 10 and 14, the Tsallis entropy values remain constant.

3.4 Order Statistics

The CDF and PDF of the kth order statistic $X_{(k)}$ from a random sample $X_1, X_2, \ldots, X_n$ with a common CDF $G(x)$ are given by:

$$\begin{aligned} G_{X_{(k)}}(x) &= \sum_{j=k}^{n} \binom{n}{j} [G(x)]^j [1 - G(x)]^{n-j} \\ &= \sum_{j=k}^{n} \binom{n}{j} \left[\frac{1}{\psi}\left(1 + \alpha + e^{-(\alpha+1)\lambda x} - (\alpha+2)e^{-\lambda x}\right)\right]^j \\ &\quad \left[1 - \frac{1}{\psi}\left(1 + \alpha + e^{-(\alpha+1)\lambda x} - (\alpha+2)e^{-\lambda x}\right)\right]^{n-j}, \end{aligned} \tag{12}$$

and

$$\begin{aligned} g_{X_{(k)}}(x) &= \tfrac{n!}{(k-1)!(n-k)!}[G(x)]^{k-1}[1 - G(x)]^{n-k} g(x) \\ &= \tfrac{n!}{(k-1)!(n-k)!}\left[\tfrac{1}{\psi}\left(1 + \alpha + e^{-(\alpha+1)\lambda x} - (\alpha+2)e^{-\lambda x}\right)\right]^{k-1} \\ &\quad \left[1 - \tfrac{1}{\psi}\left(1 + \alpha + e^{-(\alpha+1)\lambda x} - (\alpha+2)e^{-\lambda x}\right)\right]^{n-k} \\ &\quad \tfrac{1}{\psi}\left((\alpha+1)\lambda e^{-\lambda x}\left(\tfrac{\alpha+2}{\alpha+1} - e^{-\alpha\lambda x}\right)\right), \quad 0 < x \le b, \alpha, b, \lambda > 0, \end{aligned} \tag{13}$$

where $\psi = 1 + \alpha + e^{-(\alpha+1)b\lambda} - (\alpha+2)e^{-b\lambda}$. The PDf of the minimum and maximum order statistics are given by:

$$g_{X_{(1)}}(x) = \frac{\lambda n\left(-\alpha + (\alpha+2)e^{\alpha\lambda x} - 1\right) e^{\lambda((\alpha+2)b+x)}\left(1 - \dfrac{\alpha + e^{(\alpha+1)\lambda(-x)} - (\alpha+2)e^{\lambda(-x)} + 1}{\alpha + e^{(\alpha+1)(-b)\lambda} - (\alpha+2)e^{-b\lambda} + 1}\right)^n}{(\alpha+2)\left(-e^{\lambda(\alpha(b+x)+2b+x)}\right) + (\alpha+2)e^{\lambda(\alpha(b+x)+b+2x)} + e^{\lambda((\alpha+2)b+x)} - e^{\lambda(b+(\alpha+2)x)}},$$

$$g_{X_{(n)}}(x) = \frac{\lambda n e^{\lambda x}\left(-\alpha+(\alpha+2)e^{\alpha\lambda x}-1\right)\left(\frac{\alpha+e^{(\alpha+1)\lambda(-x)}-(\alpha+2)e^{\lambda(-x)}+1}{\alpha+e^{(\alpha+1)(-b)\lambda}-(\alpha+2)e^{-b\lambda}+1}\right)^{n}}{(\alpha+1)e^{(\alpha+2)\lambda x}-(\alpha+2)e^{(\alpha+1)\lambda x}+e^{\lambda x}}.$$

3.5 Mean Residual Life Function, Mean Inactivity Time, and Vitality Function

The mean residual life (MRL) function, the mean inactivity time (MIT), and the vitality function respectively are defined as

$$MRL(t) = E\left(X-t|X>t\right) = \frac{1}{1-G(t)}\int_{t}^{\infty}\left(1-G(x)\right)dx$$

$$= \frac{1}{\wp}\left((b-t)\,\psi(\alpha+1)\lambda - \begin{Bmatrix}(\alpha+1)\lambda\,(\alpha b+b-\alpha t-t)\\ -(\alpha+1)(\alpha+2)\left(e^{-\lambda t}-e^{-b\lambda}\right)\\ -e^{-(\alpha+1)b\lambda}+e^{-(\alpha+1)\lambda t}\end{Bmatrix}\right), \tag{14}$$

where $\wp = (\alpha+1)\lambda\left[\psi-\left(\alpha+e^{-(\alpha+1)\lambda t}-(\alpha+2)e^{-\lambda t}+1\right)\right], \psi = 1+\alpha+e^{-(\alpha+1)b\lambda}-(\alpha+2)e^{-b\lambda}$.

$$MIT(t) = t - E\left[X|x\leqslant t\right] = t - \frac{1}{G(t)}\int_{0}^{t} x\,g(x)dx$$

$$= \frac{e^{t\lambda}\begin{pmatrix}-e^{(\alpha+1)\lambda t}(\alpha(\alpha+3)+1)-(\alpha+1)\lambda t\\ +(\alpha+1)(\alpha+2)(\lambda t+1)e^{\alpha\lambda t}-1\end{pmatrix}}{\lambda(\alpha+1)\left[\left((\alpha+1)e^{t\lambda}-\alpha-2\right)e^{(\alpha+1)\lambda t}+e^{t\lambda}\right]}+t, \tag{15}$$

and

$$VF(t) = E\left[X|x\geq t\right] = \frac{1}{1-G(t)}\int_{0}^{\infty} x\,g(x)dx$$

$$= \frac{1}{1-G(t)}\frac{\begin{pmatrix}e^{-b(1+\alpha)\lambda}\left(1+b\,(1+\alpha)\,\lambda-e^{b\alpha\lambda}\,(1+\alpha)\,(2+\alpha)\,(1+b\lambda)\right)\\ +e^{-t(1+\alpha)\lambda}\left(\mathrm{e}^{t\alpha\lambda}\,(1+\alpha)\,(2+\alpha)\,(1+t\lambda)-1-t\,(1+\alpha)\,\lambda\right)\end{pmatrix}}{(1+\alpha)\left(1+e^{-b(1+\alpha)\lambda}+\alpha-e^{-b\lambda}\,(2+\alpha)\right)\lambda}. \tag{16}$$

4 Estimation Methods

It is well known that the properties of maximum likelihood estimators are not consistently reliable in small samples. Consequently, both conventional and modern estimation approaches have been proposed in recent years. This section examines several techniques for estimating the parameters of the proposed model, including maximum likelihood estimation, least squares and weighted least squares methods, the maximum product of spacings method, and goodness-of-fit-based approaches such as the Cramér-von Mises, Anderson-Darling, and right- and left-tail Anderson-Darling methods. In addition, a Monte Carlo simulation study is carried out to assess the performance of these estimation techniques.

4.1 Maximum Likelihood Estimation

The likelihood function for a random variable X is given by the joint PDF of the observed data. If $X_1, X_2, \ldots, X_n$ are independent and identically distributed (i.i.d.) observations from the given PDF

in Eq. (5). Then, the likelihood function for a sample of size n is:

$$L(\alpha,\lambda) = \prod_{i=1}^{n} f(x_i;\alpha,\lambda)$$
$$= \left(\frac{(1+\alpha)\lambda}{1+e^{-b(1+\alpha)\lambda}+\alpha-e^{-b\lambda}(2+\alpha)}\right)^n \prod_{i=1}^{n} e^{-x_i\lambda}\left(-e^{-x_i\alpha\lambda}+\frac{2+\alpha}{1+\alpha}\right),$$

with its Log-Likelihood:

$$\log L(\alpha,\lambda) = n\log\left(\frac{(1+\alpha)\lambda}{1+e^{-b(1+\alpha)\lambda}+\alpha-e^{-b\lambda}(2+\alpha)}\right)$$
$$+\sum_{i=1}^{n}\left[-x_i\lambda+\log\left(-e^{-x_i\alpha\lambda}+\frac{2+\alpha}{1+\alpha}\right)\right]. \tag{17}$$

To find the MLEs for $\widehat{\alpha}$, $\widehat{\lambda}$ and $\widehat{b}$, we differentiate this function with respect to α, λ and b, then set the derivatives to zero as:

$$\frac{\partial \log L}{\partial\lambda} = \frac{n}{\lambda}+\frac{n(1+\alpha)b\left[(1+\alpha)e^{-b(1+\alpha)\lambda}-(2+\alpha)e^{-b\lambda}\right]}{1+e^{-b(1+\alpha)\lambda}+\alpha-e^{-b\lambda}(2+\alpha)} = 0,$$

$$\frac{\partial \log L}{\partial\alpha} = \sum_{i=1}^{n}\frac{x_i\lambda e^{-x_i\alpha\lambda}-\frac{1}{(1+\alpha)^2}}{-e^{-x_i\alpha\lambda}+\frac{2+\alpha}{1+\alpha}}+\frac{n}{1+\alpha}-\frac{n\left(-b\lambda e^{-b(1+\alpha)\lambda}+1-e^{-b\lambda}\right)}{1+e^{-b(1+\alpha)\lambda}+\alpha-e^{-b\lambda}(2+\alpha)} = 0,$$

and

$$\frac{\partial \log L}{\partial\, b} = -\frac{n(-\lambda(\alpha+1)e^{-\lambda(\alpha+1)b}+(\alpha+2)\lambda e^{-\lambda b}}{1+2\alpha+e^{-\lambda(\alpha+1)b}-(\alpha+2)e^{-\lambda b}} = 0.$$

Solve for α, λ and b numerically using the Newton-Raphson method or gradient-based optimization, since the equations are non-linear.

4.2 Least Squares and Weighted Least Squares Methods

Since closed-form expressions of maximum likelihood estimators are not always attainable, alternative approaches have been developed to overcome this limitation. Among these, the least squares (LS) and weighted least squares (WLS) methods are well-established techniques for parameter estimation Swain et al. [22]. In this study, we consider two such strategies for estimating the parameters of the TrMWED distribution. Let $x_1, x_2, \ldots, x_n$ represent the ordered observations derived from a sample of size n from the TrMWED distribution. By determining the minimum of the function

$$S(\varpi) = \sum_{i=1}^{n}\eta_i\left\{\frac{1}{\psi}\left[1+\alpha+e^{-\lambda(\alpha+1)x_i}-(\alpha+2)e^{-\alpha\lambda x_i}\right]-\frac{i}{n+1}\right\}^2,$$

with respect to α, λ and b respectively, the LS estimates $\widehat{\alpha}_{LSE}$, $\widehat{\lambda}_{LSE}$ and $\widehat{b}_{LSE}$ can be obtained by setting $\eta_i = 1$, while we can obtain the WLS estimates $\widehat{\alpha}_{WLS}$, $\widehat{\lambda}_{WLS}$ and $\widehat{b}_{WLS}$ by setting $\eta_i = \dfrac{(n+1)^2(n+2)}{i(n-i+1)}$.

These estimates can also be obtained by solving the following equations:

$$\frac{\partial S(\varpi)}{\partial \alpha} = \sum_{i=1}^{n} \eta_i \left\{ \frac{1}{\psi} \left[1 + \alpha + e^{-\lambda(\alpha+1)x_i} - (\alpha+2)e^{-\alpha\lambda x_i} \right] - \frac{i}{n+1} \right\} \varphi_1(x_i, \psi) = 0,$$

$$\frac{\partial S(\varpi)}{\partial \lambda} = \sum_{i=1}^{n} \eta_i \left\{ \frac{1}{\psi} \left[1 + \alpha + e^{-\lambda(\alpha+1)x_i} - (\alpha+2)e^{-\alpha\lambda x_i} \right] - \frac{i}{n+1} \right\} \varphi_2(x_i, \psi) = 0,$$

$$\frac{\partial S(\varpi)}{\partial b} = \sum_{i=1}^{n} \eta_i \left\{ \frac{1}{\psi} \left[1 + \alpha + e^{-\lambda(\alpha+1)x_i} - (\alpha+2)e^{-\alpha\lambda x_i} \right] - \frac{i}{n+1} \right\} \varphi_3(x_i, \Psi) = 0,$$

where

$$\varphi_1(x_i, \varpi) = \frac{1 - \lambda x_i e^{-\lambda(\alpha+1)x_i} - e^{-\alpha\lambda x_i} + \lambda(\alpha+2)x_i e^{-\alpha\lambda x_i}}{\psi} - \frac{\kappa_i \left(1 - \lambda b e^{-\lambda(\alpha+1)b} - e^{-\alpha\lambda b} + \lambda(\alpha+2)b e^{-\alpha\lambda b}\right)}{\psi^2}, \tag{18}$$

$$\varphi_2(x_i, \varpi) = \frac{\kappa_i \left((1+\alpha)\, b e^{-\lambda(\alpha+1)b} - \alpha(\alpha+2) b e^{-\alpha\lambda b}\right)}{\psi^2} - \frac{(1+\alpha)\, x_i e^{-\lambda(\alpha+1)x_i} - \alpha(\alpha+2) x_i e^{-\alpha\lambda x_i}}{\psi}, \tag{19}$$

$$\varphi_3(x_i, \varpi) = \frac{\kappa_i((\alpha+2)\lambda e^{-\lambda b} - \lambda(\alpha+1)e^{-\lambda(\alpha+1)b}}{(1+\alpha+e^{-\lambda(\alpha+1)b} - (\alpha+2)e^{-\lambda b})^2}, \tag{20}$$

where

$$\kappa_i = 1 + \alpha + e^{-\lambda(\alpha+1)x_i} - (\alpha+2)e^{-\alpha\lambda x_i},$$

$$\psi = 1 + \alpha + e^{-(\alpha+1)b\lambda} - (\alpha+2)e^{-b\lambda}.$$

4.3 Maximum Product of Spacing Method

Cheng and Amin [23] propose that the maximum product of spacing (MPS) serves as an estimation approach comparable in interest to that of maximum likelihood estimation (MLE), based on the differences in the cumulative distribution function (cdf) values at consecutive data points. Furthermore, Al-Mofleh et al. [24] determined that the MPS estimator approach surpasses all alternative estimator methods. Uniform spacings can be defined based on a random sample of size n from a distribution with cumulative distribution function $G(x_i, \varpi)$:

$$D_i(\varpi) = G(x_i, \varpi) - G(x_{i-1}, \varpi), \quad i = 1, 2, \ldots, n, \tag{21}$$

where $G(x_0, \varpi) = 0$ and $G(x_{n+1}, \varpi) = 1$. The *MPS* estimates denoted by $\hat{\alpha}_{MPS}$, $\hat{\lambda}_{MPS}$ and $\hat{b}_{MPS}$ maximizes the function $M(\varpi)$ with respect to the unknown parameters α, λ and b:

$$M(\varpi) = \frac{1}{n+1} \sum_{i=1}^{n+1} \log D_i(\varpi)$$

$$= \frac{1}{n+1} \sum_{i=1}^{n+1} \log \left\{ \begin{array}{l} \frac{1}{\psi} \left[1 + \alpha + e^{-\lambda(\alpha+1)x_i} - (\alpha+2)e^{-\alpha\lambda x_i} \right] \\ -\frac{1}{\psi} \left[1 + \alpha + e^{-\lambda(\alpha+1)x_{i-1}} - (\alpha+2)e^{-\alpha\lambda x_{i-1}} \right] \end{array} \right\},$$

$\psi = 1 + \alpha + e^{-(\alpha+1)b\lambda} - (\alpha+2)e^{-b\lambda}$., or by solving the following equations

$$\frac{\partial M(\varpi)}{\partial \alpha} = \frac{1}{n+1}\sum_{i=1}^{n+1}\frac{\varphi_1(x_{i-1},\varpi) - \varphi_1(x_i,\varpi)}{D_i} = 0,$$

$$\frac{\partial M(\Psi)}{\partial \lambda} = \frac{1}{n+1}\sum_{i=1}^{n+1}\frac{\varphi_2(x_{i-1},\varpi) - \varphi_2(x_i,\varpi)}{D_i} = 0,$$

$$\frac{\partial M(\Psi)}{\partial b} = \frac{1}{n+1}\sum_{i=1}^{n+1}\frac{\varphi_3(x_{i-1},\varpi) - \varphi_3(x_i,\varpi)}{D_i} = 0,$$

where $\varphi_1(x_i,\varpi)$, $\varphi_2(x_i,\varpi)$ and $\varphi_3(x_i,\varpi)$ are given earlier. For more details on this method, see Cheng and Stephens [25].

4.4 Goodness-of-Fit Statistics Estimation Methods

In recent years, some writers have employed conventional goodness-of-fit statistics, such as the Cramer-Von-Mises and Anderson-Darling statistics, to generate estimators for unknown parameters. Dey et al. [26] assessed the process capability index Cpyk for Lindley and power Lindley distributions. In addition to these methodologies and this methodology, we advocate for the application of the Pearson chi-square statistic χ^2, whereby the estimators referred to as CSMM are derived by minimizing χ^2 concerning the unknown parameters.

4.4.1 Cramer-Von-Mises Method

Subsequently, Boos [27] demonstrated that the Cramer-von-Mises estimates (CMEs), derived from the distance of Cramer-von-Mises goodness-of-fit statistics, exhibit the least bias in comparison to alternative estimators. For calculation purposes, Boos [27] provides the formula $C(\varpi)$ for this statistic, wherein the estimators guarantee its minimum about the unknown parameters.

$$C(\varpi) = \frac{1}{12n} + \sum_{i=1}^{n}\left\{\frac{1}{\psi}\left[1 + \alpha + e^{-\lambda(\alpha+1)x_i} - (\alpha+2)e^{-\alpha\lambda x_i}\right] - \frac{2i-1}{2n}\right\}^2, \tag{22}$$

$\psi = 1 + \alpha + e^{-(\alpha+1)b\lambda} - (\alpha+2)e^{-b\lambda}$. They also can be obtained as the solution of the following equations:

$$\frac{\partial C(\varpi)}{\partial \alpha} = \sum_{i=1}^{n}\left\{\frac{1}{\psi}\left[1 + \alpha + e^{-\lambda(\alpha+1)x_i} - (\alpha+2)e^{-\alpha\lambda x_i}\right] - \frac{2i-1}{2n}\right\}\varphi_1(x_i,\varpi) = 0,$$

$$\frac{\partial C(\varpi)}{\partial \lambda} = \sum_{i=1}^{n}\left\{\frac{1}{\psi}\left[1 + \alpha + e^{-\lambda(\alpha+1)x_i} - (\alpha+2)e^{-\alpha\lambda x_i}\right] - \frac{2i-1}{2n}\right\}\varphi_2(x_i,\varpi) = 0$$

$$\frac{\partial C(\varpi)}{\partial b} = \sum_{i=1}^{n}\left\{\frac{1}{\psi}\left[1 + \alpha + e^{-\lambda(\alpha+1)x_i} - (\alpha+2)e^{-\alpha\lambda x_i}\right] - \frac{2i-1}{2n}\right\}\varphi_3(x_i,\varpi) = 0.$$

4.4.2 Anderson-Darling Method

The Anderson-Darling estimation method (ADE) is based on the classical goodness-of-fit statistic test (AD) proposed by Anderson and Darling [28]. Basically, this statistic is used to fit data to a

theoretical hypothesized model G_0. When the parameters are unknown, they can be estimated by $\widehat{\alpha}_{ADE}$, $\widehat{\lambda}_{ADE}$ and $\widehat{b}_{ADE}$which minimize the (AD) statistic given in the form:

$$ADE(\varpi) = -n - n^{-1}\sum_{i=1}^{n}(2i-1)\left\{\log G(x_i) + \log\left(1 - G(x_{-i+n+1})\right)\right\},$$

which is tantamount to nullifying the first derivatives of this function concerning α, λ and b. For further information regarding this strategy, one may refer to Boos [27]. Rodrigues et al. [29] demonstrated that the ADE estimation approach yields the most efficient estimators. The Anderson-Darling statistic emphasizes the tails of the distribution; therefore, for right or left-tailed distributions, the right tail (ADE_{R-T}) and left tail (ADE_{L-T}) Anderson-Darling estimators are employed in recent literature Rodrigues et al. [29], Dey et al. [26]. Conversely, Akgül [30] proved that the minimal distance technique estimation ADE is a very competitive approach in comparison to ML estimation. Furthermore, Ibrahim [24] validated the preeminence of this approach.

4.4.3 Right and Left Tails Anderson-Darling Methods

It is well known that the Anderson-Darling statistic gives more weight for the tails of the distribution, so for right or left tailed distributions, right tail (ADE_{R-T}) and left tail (ADE_{L-T}) Anderson-Darling estimators are proposed to estimate the unknown parameters like in Rodrigues et al. [29] and Dey et al. [26]. The $(ADE_{R-T})\widehat{\alpha}_{ADE_{(R-T)}}$, $\widehat{\lambda}_{ADE_{(R-T)}}$ and $\widehat{b}_{ADE_{(R-T)}}$ are obtained by minimizing

$$ADE_{(R-T)}(\varpi) = \frac{n}{2} - 2\sum_{i=1}^{n}\log G(x_i) - \frac{1}{n}\sum_{i=1}^{n}(2i-1)\log\left\{1 - G(x_{-i+n+1})\right\},$$

or

$$\frac{\partial}{\partial\alpha}\left[ADE_{(R-T)}(\varpi)\right] = 0, \quad \frac{\partial}{\partial\lambda}\left[ADE_{(R-T)}(\varpi)\right] = 0, \quad \frac{\partial}{\partial\, b}\left[ADE_{(R-T)}(\varpi)\right] = 0.$$

And the $(ADE_{L-T})\widehat{\alpha}_{ADE_{(L-T)}}$, $\widehat{\lambda}_{ADE_{(L-T)}}$ and $\widehat{b}_{ADE_{(L-T)}}$ are obtained by minimizing

$$ADE_{(L-T)}(\varpi) = -\frac{3}{2}n + 2\sum_{i=1}^{n}G(x_i) - \frac{1}{n}\sum_{i=1}^{n}(2i-1)\log\left\{G(x_i)\right\},$$

or

$$\frac{\partial}{\partial\alpha}\left[ADE_{(L-T)}(\varpi)\right] = 0, \quad \frac{\partial}{\partial\lambda}\left[ADE_{(L-T)}(\varpi)\right] = 0, \quad \frac{\partial}{\partial\, b}\left[ADE_{(L-T)}(\varpi)\right] = 0,$$

with respect to the unknown parameters.

5 Monte Carlo Simulations

A theoretical comparison of the performance of the estimators discussed in the preceding sections is not feasible; therefore, a Monte Carlo simulation study is conducted to determine the optimal estimation method among eight traditional techniques. We generate 10,000 random samples under varying sample sizes and parameter values, repeating the procedure 1000 times. For each iteration, the average estimates and mean squared errors are calculated. The results are reported in Table 3 for sample sizes $n = 15, 35, 100$ and in Table 4 for $n = 250, 500$, in terms of the Average Estimator (AE),

Average Width (AW), and Mean Squared Error (MSE), where

$$AE(\hat{\mathbb{Z}}) = \frac{1}{10,000}\sum_{i=1}^{10,000}\hat{\mathbb{Z}}_i, \text{ and } MSE(\hat{\mathbb{Z}}) = \frac{1}{10,000}\sum_{i=1}^{10,000}(\hat{\mathbb{Z}} - \mathbb{Z})^2, \text{ where } \mathbb{Z} = \alpha, b, \lambda.$$

Table 3: AE, (MSE) and AW values of α, λ and b, with different estimation methods for $n = 15, 35, 100$

Method	$\alpha = 2$	AW	$\lambda = 4$	AW	$b = 1.5$	AW
		$n = 15$				
MLE	1.8632 (0.0056)	10.97e−3	4.1144 (0.0055)	10.78e−3	1.4559 (0.0059)	11.5e−3
WLS	1.7486 (0.0075)	14.70e−3	3.8724 (0.0071)	13.91e−3	1.4458 (0.0071)	13.9e−3
MPS	2.1512 (0.0069)	13.52e−3	4.1257 (0.0062)	12.15e−3	1.4484 (0.0063)	12.3e−3
CMEs	1.6938 (0.0094)	18.42e−3	3.8018 (0.0092)	18.02e−3	1.4383 (0.0090)	17.2e−3
LSE	2.1582 (0.0081)	15.87e−3	3.8388 (0.0080)	15.68e−3	1.4397 (0.0082)	16.3e−3
ADE	1.6663 (0.0107)	20.97e−3	4.1311 (0.0099)	19.40e−3	1.4338 (0.0097)	19.4e−3
ADE_{L-R}	2.1519 (0.0109)	21.30e−3	4.1403 (0.0107)	20.91e−3	1.4305 (0.0103)	20.1e−3
ADE_{L-T}	2.1567 (0.0111)	21.75e−3	4.1545 (0.0114)	22.30e−3	1.4286 (0.0109)	21.3e−3
		$n = 35$				
MLE	1.8953 (0.0042)	8.2e−3	4.0898 (0.0047)	9.21e−3	1.4685 (0.0048)	9.4e−3
WLS	1.7831 (0.0061)	11.9e−3	3.9039 (0.0059)	11.56e−3	1.4584 (0.0063)	12.3e−3
MPS	2.1193 (0.0058)	11.3e−3	4.1011 (0.0049)	9.6e−3	1.4613 (0.0055)	10.7e−3
CMEs	1.7258 (0.0079)	15.4e−3	3.8252 (0.0081)	15.87e−3	1.4506 (0.0082)	16.2e−3
LSE	2.1263 (0.0066)	12.9e−3	3.8418 (0.0068)	13.3e−3	1.4523 (0.0074)	14.5e−3
ADE	1.7018 (0.0092)	18.1e−3	4.1065 (0.0087)	17.05e−3	1.4464 (0.0089)	17.4e−3
ADE_{L-R}	2.1285 (0.0096)	18.8e−3	4.1239 (0.0095)	18.62e−3	1.4431 (0.0095)	18.6e−3
ADE_{L-T}	2.1333 (0.0100)	19.6e−3	4.1309 (0.0102)	19.99e−3	1.4412 (0.0106)	20.7e−3
		$n = 100$				
MLE	1.9425 (0.0029)	5.68e−3	4.0549 (0.0028)	5.48e−3	1.4817 (0.0035)	6.8e−3
WLS	1.8298 (0.0048)	9.40e−3	3.9284 (0.0044)	8.62e−3	1.4716 (0.0051)	9.8e−3
MPS	2.0756 (0.0043)	8.42e−3	4.0662 (0.0034)	6.66e−3	1.4742 (0.0042)	8.2e−3
CMEs	1.7965 (0.0067)	13.13e−3	3.8601 (0.0065)	12.74e−3	1.4638 (0.0069)	13.5e−3
LSE	2.0826 (0.0053)	10.38e−3	3.8668 (0.0053)	10.38e−3	1.4655 (0.0061)	11.9e−3
ADE	1.7475 (0.0079)	15.48e−3	4.0749 (0.0072)	14.11e−3	1.4596 (0.0076)	14.8e−3
ADE_{L-R}	2.0863 (0.0085)	16.66e−3	4.0978 (0.0082)	16.07e−3	1.4563 (0.0082)	16.1e−3
ADE_{L-T}	2.0911 (0.0089)	17.44e−3	4.0994 (0.0089)	17.44e−3	1.4544 (0.0093)	18.2e−3

Table 4: AE, (MSE) and AW values of α, λ and b, with different estimation methods for $n = 250, 500$

Method	$\alpha = 2$	AW	$\lambda = 4$	AW	$b = 1.5$	AW
		$n = 250$				
MLE	1.9659(0.0021)	4.11e–3	4.0288(0.0017)	3.3e–3	1.4893(0.0024)	4.7e–3
WLS	1.8532(0.0041)	8.03e–3	3.9595(0.0033)	6.4e–3	1.4792(0.0039)	7.64e–3
MPS	2.0522(0.0034)	6.66e–3	4.0401(0.0023)	4.5e–3	1.4818(0.0031)	6.07e–3
CMEs	1.7731(0.0058)	11.36e–3	3.8862(0.0054)	10.5e–3	1.4714(0.0058)	11.3e–3
LSE	2.0592(0.0047)	8.03e–3	3.8929(0.0045)	8.8e–3	1.4731(0.0051)	9.8e–3
ADE	1.7809(0.0067)	13.13e–3	4.0488(0.0061)	11.7e–3	1.4372(0.0065)	12.7e–3
ADE_{L-R}	2.0649(0.0074)	14.50e–3	4.0662(0.0073)	14.3e–3	1.4639(0.0071)	13.9e–3
ADE_{L-T}	2.0697(0.0086)	16.89e–3	4.0679(0.0081)	15.8e–3	1.4621(0.0082)	16.1e–3
		$n = 500$				
	$\alpha = 2$	AW	$\lambda = 4$	AW	b = 1.5	AW
MLE	1.9834(0.0012)	2.3e–3	4.0124(0.0009)	1.7e–3	1.4977(0.0015)	2.94e–3
WLS	1.8747(0.0034)	6.1e–3	3.9742(0.0025)	4.9e–3	1.4876(0.0030)	5.88e–3
MPS	2.0347(0.0023)	4.5e–3	4.0237(0.0015)	2.9e–3	1.4902(0.0022)	4.32e–3
CMEs	1.8140(0.0047)	9.2e–3	3.8977(0.0046)	9.1e–3	1.4798(0.0049)	9.6e–3
LSE	2.0417(0.0038)	7.4e–3	3.9044(0.0032)	6.2e–3	1.4815(0.0041)	8.03e–3
ADE	1.7924(0.0058)	11.3e–3	4.0324(0.0051)	9.9e–3	1.4756(0.0056)	1.09e–3
ADE_{L-R}	2.0534(0.0065)	12.7e–3	4.0416(0.0062)	12.1e–3	1.4723(0.0062)	1.21e–3
ADE_{L-T}	2.0582(0.0072)	14.1e–3	4.0533(0.0069)	13.5e–3	1.4704(0.0073)	1.43e–3

Fig. 6 summarizes the MSE values, illustrating the trend of each estimator across different sample sizes for the parameter settings $\alpha = 2, \lambda = 4, b = 1.5$. The following observations are drawn from the estimation results of obtained using various methods across the considered sample sizes:

- **MLE:** The maximum likelihood estimator provides estimates of α, λ, and b that are closest to the true values ($\alpha = 2$, $\lambda = 4$, $b = 1.5$) across all sample sizes. Accuracy improves with increasing n, as reflected by smaller standard errors. For example, at $n = 15$, $\alpha = 1.8632$ (MSE $= 0.0056$), $\lambda = 4.1144$ (MSE $= 0.0055$), and $b = 1.4559$ (MSE $= 0.0059$). At $n = 500$, the estimates improve to $\alpha = 1.9834$ (MSE $= 0.0012$), $\lambda = 4.0124$ (MSE $= 0.0009$), and $b = 1.4893$ (MSE $= 0.0024$), demonstrating the efficiency and robustness of MLE.
- **WLS:** Weighted least squares generally produces slightly biased estimates, typically underestimating the true parameters. Accuracy improves with larger sample sizes, but a noticeable bias remains. For instance, with $n = 15$, the bias is more pronounced, while at $n = 500$, the estimates are more accurate but still fall short of MLE's performance.
- **MPS:** The maximum product of spacings method tends to overestimate α, λ, and b, especially for smaller sample sizes. Standard errors decrease as n increases, indicating improved precision. By $n = 100$ and $n = 250$, estimates stabilize, though some bias persists despite the improved accuracy.
- **CMEs:** The Cramér-von Mises estimators often underestimate α, λ, and b, particularly at small n, exhibiting relatively high bias and larger standard errors. While performance improves as the

sample size grows, CMEs remain less accurate than MLE. For example, at $n = 15$, substantial underestimation occurs, and even at $n = 500$, precision is still inferior to MLE.

- **LSE:** Least squares estimation shows bias, particularly for λ, which tends to be underestimated. Accuracy improves with larger sample sizes, but LSE does not match the performance of MLE or ADE-based methods.
- **ADE:** The adjusted density estimator generally yields estimates closer to the true parameters than most other methods, with standard errors decreasing as n increases. At $n = 15$, ADE provides relatively accurate estimates with reduced bias and lower standard errors (excluding MLE). At $n = 500$, ADE gives the second-most accurate estimates after MLE, e.g., $\alpha = 1.7924$ (SE $= 0.0058$) and $\lambda = 4.0324$ (SE $= 0.0051$).
- **$\mathbf{ADE}_{L-R}$ and $\mathbf{ADE}_{L-T}$:** These adjusted ADE methods offer marginal improvements over standard ADE. At small n (e.g., $n = 15$), the adjustments have little effect, but the improvements become more noticeable at larger sample sizes ($n = 250$ and $n = 500$). Nevertheless, they still do not reach MLE's level of accuracy.
- **In general,** the tables show that MLE outperforms all other techniques in terms of mean squared error (MSE). MPS ranks second, followed by WLS, LSE, CMEs, ADE, ADE_{L-R}, and ADE_{L-T}. Across all methods, MSE decreases as sample size increases, confirming consistency. Additionally, MLE yields the narrowest absolute widths (AWs) for estimating α, λ, and b, highlighting its superior performance.

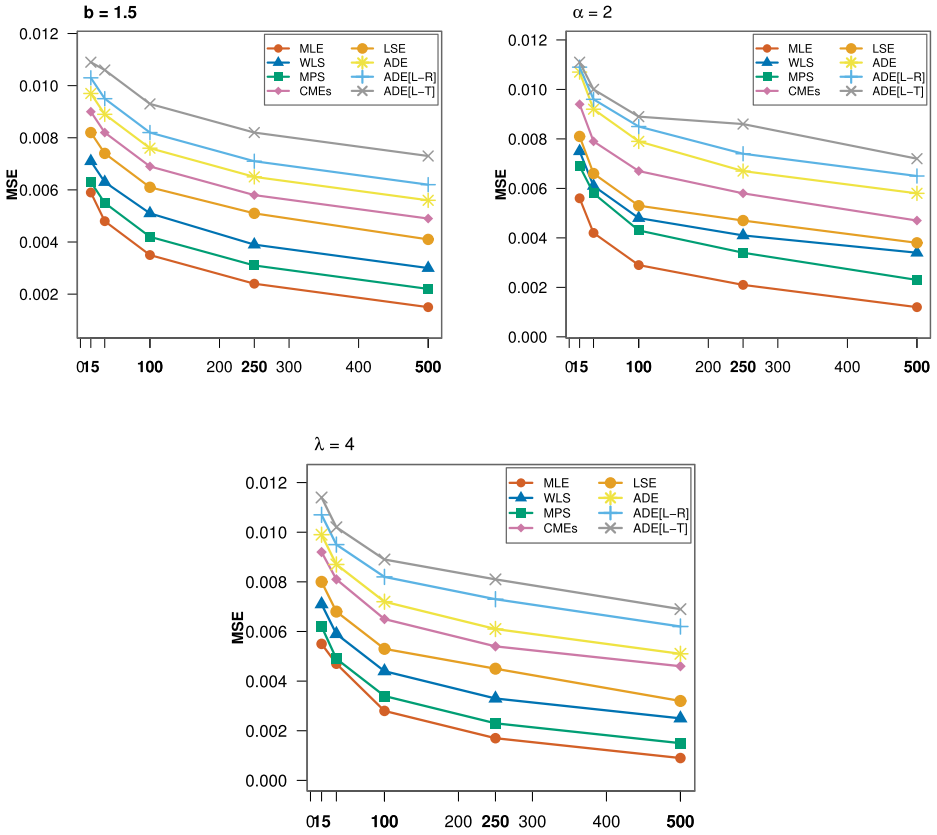

Figure 6: MSE values of different estimators of the TrMWED for $\lambda = 4, \alpha = 2, b = 1.5, n = 15, 35, 100, 250, 500$

Table 5 summary summarizes the main results obtained through this simulation for all cases considered in this study.

Table 5: Summary of estimator performance across sample sizes

Method	Small $n = 15$	Medium $n = 100$	Large $n = 500$
MLE	Best overall	Best overall	Best overall
MPS	↑ Overestimates α	↑ Slight bias	↑ Slight bias
WLS	↓ Underestimates α, λ	Stable	Stable
LSE	↑ Overestimates α	↑ Bias persists	↑ Bias persists
CMEs	↓ Consistently low	↓ Low	↓ Low
ADE variants	Mixed, high variance	Mixed	Mixed

6 Applications of Real Data

In this section, three real datasets are analyzed to assess the applicability of the proposed distribution. These datasets include wind speed data from Annaba, Algeria; glycated hemoglobin levels of patients in Algeria; and COVID-19 data from the United Kingdom. The performance of the new distribution is compared to several existing models, namely the exponentiated Weibull (EW) proposed by Pal et al. [31], the exponential flexible Weibull extension (EFWE) suggested by El-Desouky et al. [32], the power Quasi-Lindley Distribution (PQLD) introduced by Alkarni [33], and the transmuted inverse Rayleigh distribution (TIRD) proposed by Shala and Merovci [34], unit generalized inverse Weibull distribution (UGIWD), Topp-Leone extended exponential distribution (TL-EE), The truncated generalized Fréchet power (TGFrP), and truncated log-logistic exponential (TLLE) distribution, with their respective PDFs defined as follows:

$$f(x;\alpha,\gamma,\lambda) = \alpha\gamma\lambda^{\gamma}x^{\gamma-1}[1-\exp\{-(\lambda x)^{\gamma}\}]^{\alpha-1}\exp\{-(\lambda x)^{\gamma}\}, \quad x>0,\alpha,\gamma,\lambda>0,$$

$$f(x;\alpha,\beta,\lambda) = \lambda\left(\alpha+\frac{\beta}{x^2}\right)e^{\alpha x-\frac{\beta}{x}}e^{e^{\alpha x-\frac{\beta}{x}}}\exp\left\{-\lambda e^{\alpha-\frac{\beta}{x}}\right\}, x>0,\beta,\alpha,\lambda>0,$$

$$f(x;\theta,\beta,\alpha) = \frac{\alpha\theta}{\beta+1}(\beta+\theta x^{\alpha})x^{\alpha-1}e^{-\theta x^{\alpha}}, \quad \theta,\alpha,\beta,x>0,$$

$$f(x;\theta,\beta,\alpha) = \frac{\alpha\theta}{\beta+1}(\beta+\theta x^{\alpha})x^{\alpha-1}e^{-\theta x^{\alpha}}, \quad \theta,\alpha,\beta,x>0,$$

$$f(x;\lambda,\alpha,\sigma) = \frac{2\alpha(1+\lambda)\sigma^2}{x^3}e^{-\alpha\left(\frac{\sigma}{x}\right)^2} - \frac{4\alpha\lambda\sigma^2}{x^3}e^{-2\alpha\left(\frac{\sigma}{x}\right)^2}, x\geq 0,\sigma,\alpha,|\lambda|\leq 1,$$

$$f(x;\lambda,\alpha,\beta) = \frac{\alpha\lambda\beta}{x^2}\left(\frac{\lambda(1-x)}{x}\right)^{\beta-1}\exp\left\{-\alpha\left(\frac{\lambda(1-x)}{x}\right)^{\beta}\right\}, 0<x<1, \alpha,\beta,\lambda>0,$$

$$f(x;\alpha,\beta,\lambda) = 2\alpha\beta\lambda\,(1+\alpha x)^{\beta-1}\,e^{2\left\{1-(1+\alpha x)^{\beta}\right\}}\left\{1-e^{2\left\{1-(1+\alpha x)^{\beta}\right\}}\right\}^{\lambda-1},$$

$$f(x,\alpha,\beta,\lambda) = \frac{\alpha\beta\lambda x^{-\lambda-1}e^{-\alpha x^{-\lambda}}\,(1-e^{-\alpha})^{\beta-1}}{1-(1-e^{-\alpha})^{\beta}},$$

$$f(x;\alpha,\beta,\lambda) = \frac{\alpha\,(1+\beta)\,\lambda e^{-\lambda x}\,(1-e^{-\lambda x})^{\alpha-1}}{\{1+\beta\,(1-e^{-\lambda x})^{\alpha}\}^2}.$$

The distribution parameters are estimated using the maximum likelihood method, along with the calculation of the negative maximized log-likelihood (MLL), Akaike Information Criterion (AIC), Consistent Akaike Information Criterion (CAIC), Bayesian Information Criterion (BIC), Hannan-Quinn Information Criterion (HQIC), and the Kolmogorov-Smirnov (KS) test statistic with its corresponding p-value. For assessing model fit, the best-fitting distribution is identified as the one with the lowest values of KS, AIC, BIC, CAIC, and HQIC. which are defined as follows:

$$\text{BIC} = -2\ell + k\,\ln(n), \quad \text{AIC} = -2\ell + 2k, \quad \text{HQIC} = 2k\ln\left[\ln(n)\right] - 2\ell, \quad \text{CAIC} = -2\ell + \frac{2k\,n}{n-k-1},$$

where ℓ represents the negative maximized log-likelihood, n denotes the sample size, and z is the number of parameters. Let $X_1, X_2, \ldots, X_n$ be a random sample from a continuous distribution with cumulative distribution function (CDF) $F(x)$. The empirical distribution function (EDF), $F_n(x)$, is defined as: $F_n(x) = \frac{1}{n}\sum_{i=1}^{n} \mathbf{1}_{\{X_i \le x\}}$ The Kolmogorov–Smirnov test statistic is:

$$D_n = \sup_x |F_n(x) - F(x)|,$$

where sup denotes the supremum over all x. The null and alternative hypotheses are:

$$H_0 : F(x) = F_0(x), \quad \text{for all } x, \text{and } H_1 : F(x) \neq F_0(x), \quad \text{for some } x.$$

That is, the sample comes from the distribution $F_0(x)$. The test rejects H_0 if $D_n > D_\alpha$, where D_α is the critical value at significance level α. The MLE of the TrMWED parameters are considered as the true parameters values.

Dataset I: Wind speed

Monthly and annual data (2000–2008) of wind speed measured at 10 m height and collected by the meteorological station at Rabah Bitat International Airport, Annaba, Algeria. The data are presented in Table 6 below.

Table 6: Monthly data from 2000 to 2008

	2000	2001	2002	2003	2004	2005	2006	2007	2008
Jan	3.6	4.1	3.6	4.9	4.7	4.7	3.7	2.9	3.1
Feb	4.1	4.0	3.7	3.9	3.6	5.7	3.9	4.1	2.9
Mar	4.0	3.8	3.8	3.5	3.5	3.7	4.7	4.6	3.6
Apr	3.9	4.1	3.6	3.9	3.7	3.7	3.9	3.4	4.0
May	3.2	3.5	4.1	3.5	4.0	3.2	3.7	3.9	3.6
Jun	3.6	3.6	3.7	3.8	4.1	2.9	4.1	3.9	3.8
Jul	3.4	4.0	3.8	4.0	4.0	4.2	3.8	4.1	5.4
Aug	3.6	3.6	3.4	3.9	3.7	4.0	4.0	4.0	4.3
Sep	3.7	3.1	3.4	4.2	3.8	3.2	3.7	3.9	3.7
Oct	3.7	2.8	3.6	3.9	2.8	3.1	3.4	3.6	3.3
Nov	4.0	3.9	4.9	3.9	3.9	3.9	3.4	3.6	3.7
Dec	3.9	4.0	4.5	4.8	4.0	4.1	3.0	4.0	3.4

Dataset II: Glycated hemoglobin levels

This part is used for a statistical study of data that represent variables involved in the health of patients with diabetes. We collected medical records of patients with autoimmune disease in Annaba, Algeria, from June 2019 to May 2021, for this purpose, and the data is given by: 11.3, 12.8, 12.2, 9, 8.6, 8.8, 8.6, 10.3, 9.6, 7, 12.5, 7.1, 7.5, 14, 13.8, 9.4, 7.1, 7.5, 9.6, 7.32, 6, 8, 10, 6.9, 7, 9, 7.5, 10, 6, 6.1, 8.62, 10.5, 7.54, 13.7, 15.5, 13.1,11.3, 11.2, 14.9, 9.4,10.6, 17.7, 12, 12.7, 15.

Dataset III: COVID-19

The third data set are the mortality rates of COVID-19 in the United Kingdom. The data set consists of values recorded over several periods, highlighting fluctuations in mortality rates. June 30, 2020. The data is retrieved from World Health Organization [35]. Also, it is considered by Kilai et al. [36] for a new generalization of Gull Alpha power family of distributions and by Kalantan et al. [37] for Chen-Burr XII mode. The data set is given by: 0.0587, 0.0863, 0.1165, 0.1247, 0.1277, 0.1303, 0.1652, 0.2079, 0.2395, 0.2845, 0.2992, 0.3188, 0.3317, 0.3446, 0.3553, 0.3622, 0.3926, 0.3926, 0.4633, 0.4690, 0.4954, 0.5139, 0.5696, 0.5837, 0.6197, 0.6365, 0.7096, 0.7444, 0.8590, 1.0438, 1.0602, 1.1305, 1.1468, 1.1533, 1.2260, 1.2707, 1.4149, 1.5709, 1.6017, 1.6083, 1.6324, 1.6998, 1.8164, 1.8392, 1.8721, 2.1360, 2.3987, 2.4153, 2.5225, 2.7087, 2.7946, 3.3609, 3.3715, 3.7840, 4.1969, 4.3451, 4.4627, 4.6477, 5.3664, 5.4500, 5.7522, 6.4241, 7.0657, 8.2307, 9.6315, 10.1870, 11.1429, 11.2019, 11.4584, 0.2751, 0.4110, 0.7193, 1.3423, 1.9844, 3.9042, 7.4456.

The descriptive statistics for the three datasets are summarized in Table 7. All three datasets exhibit right-skewness, with the degree of skewness decreasing in the order: Data Set III, Data Set I, and Data Set II. Moreover, the small difference between the mean and median in Data Sets I and II suggests relatively symmetric distributions compared to Data Set III.

Table 7: Descriptive statistics for Data Set 1, Data Set 2, and Data Set 3

Statistic	Data Set 1	Data Set 2	Data Set 3
Sample Size	108	45	76
Minimum	2.8	6	0.0587
Maximum	5.7	17.7	11.4584
Mean	3.813	10.095	2.437
Median	3.8	9.6	1.248
Standard Deviation	0.486	2.882	2.936
Variance	0.236	8.308	8.620
Skewness	0.831	0.597	1.703
Kurtosis	5.361	2.592	5.091

The density plots, boxplots, histograms, and Total Time on Test (TTT) plots, as well as the Quantile-Quantile (Q-Q) and Probability-Probability (P-P) plots for the three datasets, are presented in Figs. 7–9, respectively. The shape of the hazard rate function for each dataset is assessed graphically using the TTT method Aarset [38]. For a sample of size n, the empirical TTT plot is obtained by plotting $T(i/n)$ against i/n, where $T(i/n)$ denotes the cumulative total time on test, where

$$T(i/n) = \frac{\sum_{j=1}^{i} X_{(j)} + (n-i)X_{(i)}}{\sum_{j=1}^{n} X_{(j)}},$$

with $X_{(i)}$ as the i-th sample order statistic.

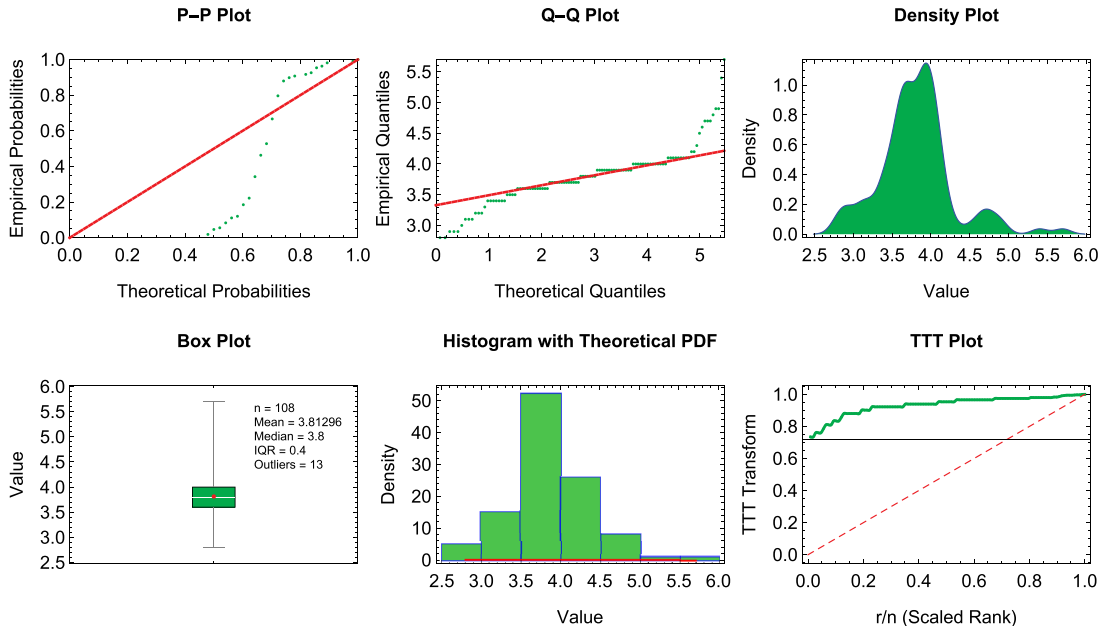

Figure 7: The Q-Q, P-P, box, density, TTT and histogram plots of the TrMWED based on Dataset I

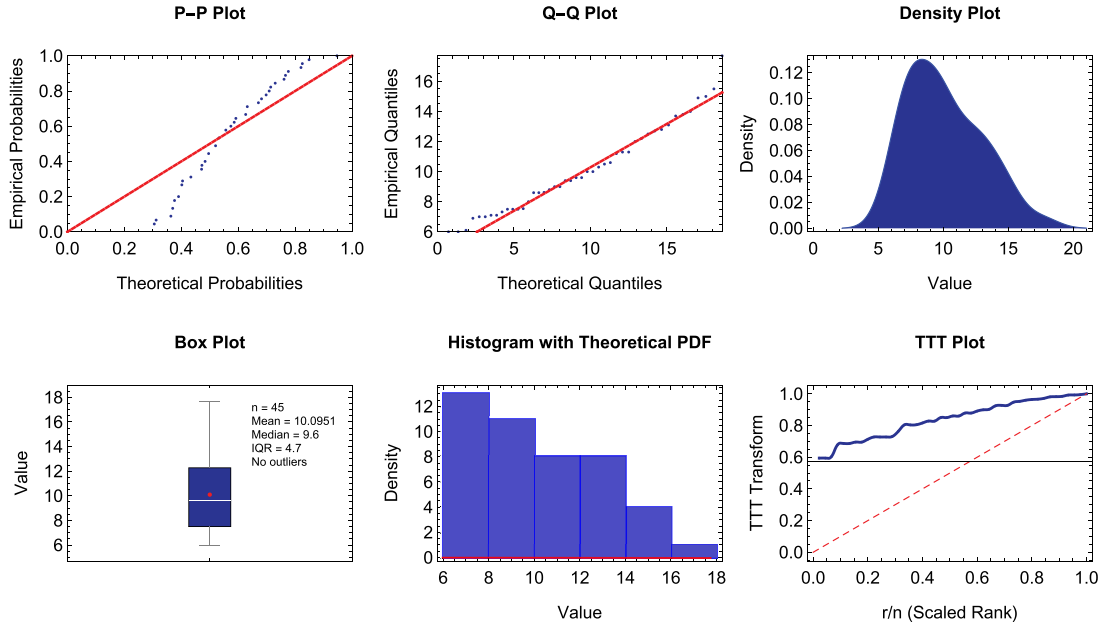

Figure 8: The Q-Q, P-P, box, density, TTT and histogram plots of the TrMWED based on Dataset II

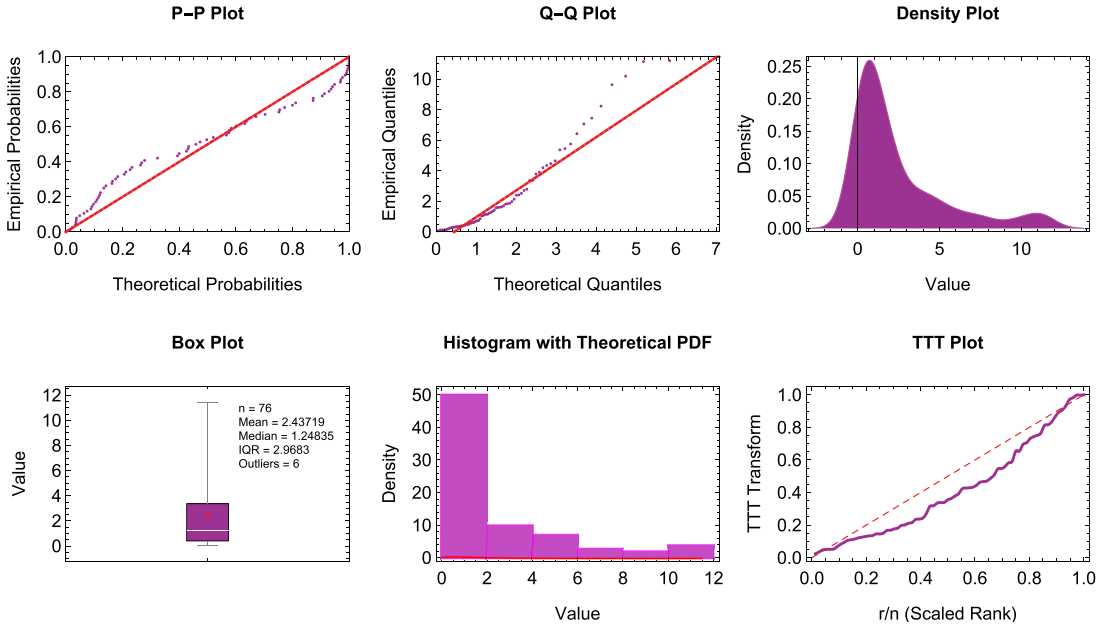

Figure 9: The Q-Q, P-P, box, density, TTT and histogram plots of the TrMWED based on Dataset III

Table 8 reports the parameter estimates of the proposed TrMWED distribution, obtained through various estimation methods for Data Sets I, II, and III.

Table 8: Estimates of parameters α, λ, and b using different estimation methods

Data Set	MLE	WLS	MPS	CMEs	LSE	ADE	$ADE_{L\text{-}R}$	$ADE_{L\text{-}T}$
				α				
I	3.1562	3.5623	3.2516	3.8491	3.7614	3.9125	4.0214	4.5236
II	2.0365	2.6748	2.4156	2.6954	2.7158	2.8956	2.9425	2.9794
III	1.9562	1.9689	1.9623	1.9802	1.9756	1.9856	1.9947	1.9988
				λ				
I	4.0253	4.4125	4.3251	4.8459	4.6642	5.0214	5.4512	5.6236
II	3.2254	3.4512	3.3176	3.6245	3.5126	3.7625	3.7841	3.8412
III	4.6251	4.6336	4.6304	4.6552	4.6401	4.6639	4.6677	4.7263
				b				
I	6.5231	6.5398	6.5321	6.5487	6.5432	6.5521	6.5569	6.5599
II	5.6231	5.6398	5.6278	5.6479	5.6453	5.6509	5.6523	5.6564
III	4.9856	4.9986	4.9921	5.0046	4.9989	5.0125	5.0189	5.0265

The following remarks can be concluded:

- The estimates for parameter b are remarkably consistent across all estimation methods for a given data set. The range of estimates is very narrow (e.g., for Data Set I, from 6.5231 to 6.5599),

indicating that the choice of estimation method has relatively little impact on b compared to α and λ.

- The estimates for λ show more variability than b but less than α. For Data Set III, estimates are quite close (4.6251 to 4.7263), indicating good agreement, whereas for Data Sets I and II, wider ranges suggest that the estimation method has a more noticeable effect on λ.
- The estimates for α exhibit the largest variation within each data set. For Data Set I, they span from 3.1562 (MLE) to 4.5236 ($ADE_{L\text{-}T}$), a substantial difference relative to the parameter magnitude. Similarly, Data Set II ranges from 2.0365 to 2.9794. This highlights that the estimation method has the most significant impact on α.
- The MLE consistently provides the lowest (or among the lowest) estimates for α and λ across all data sets. For b, MLE estimates are also generally on the lower end but remain very close to other methods. This may indicate lower bias if the true value is on the smaller side, or that other methods tend to overestimate.
- The WLS, MPS, CMEs, LSE, and ADE methods typically produce estimates in the middle range, with their relative positions varying slightly across parameters and data sets. They generally yield higher estimates than MLE, particularly for α and λ.
- The $ADE_{L\text{-}R}$ and $ADE_{L\text{-}T}$ methods, especially $ADE_{L\text{-}T}$, consistently give the highest estimates for all three parameters across all data sets. This suggests these methods may be more prone to overestimation or capture distributional aspects leading to larger parameter values.

Table 9 presents the MLEs of α and λ, the log-likelihood values, as well as the AIC, AICc, BIC, KS-statistics and p-values for the data sets considered.

Based on Table 9, the following conclusions can be drawn:

- The TrMWED model consistently produces the smallest Kolmogorov–Smirnov statistics and the highest p-values across all datasets, confirming its superior goodness-of-fit compared to the competing models. Overall, it provides the best fit, followed by the EW, EFWE, PQLD, and TIRD models in descending order of performance.
- Data Set I: The TrMWED model yields the lowest AIC (129.534), very closely followed by the EW (129.536) and EFWE (129.548) models. For the BIC, TrMWED again ranks first (137.322), slightly ahead of EW (137.376). Similarly, TrMWED achieves the lowest HQIC (132.538), with EW (132.592) a close second. Taken together, these results indicate that TrMWED provides the most favorable balance between fit and complexity, with EW remaining a strong competitor.
- Data Set II: The TrMWED model attains the lowest AIC (182.224), BIC (187.643), and HQIC (184.245) values, narrowly outperforming the EW model (182.250, 187.669, and 184.270, respectively). This further supports TrMWED as the best-fitting model for this dataset, with EW again as the closest rival.
- Data Set III: The TrMWED model secures the lowest AIC (74.052), outperforming all other models whose values exceed 76. It also records the smallest BIC (83.044), with EW (83.104) and EFWE (83.122) following closely. For HQIC, TrMWED leads once more (78.846), narrowly ahead of EW (78.906) and EFWE (78.924).
- Overall: Across all three datasets, the TrMWED model consistently demonstrates the most favorable values for AIC, BIC, and HQIC, reflecting an optimal balance between fit and parsimony. The EW and EFWE models represent the next best alternatives, with performance particularly close in Data Set III.

Table 9: MLEs, log-likelihood, information criteria, KS statistic, and p-values based on Datasets I, II, and III

Model	MLEs $(\alpha;\lambda;b)$	$-LL$	AIC	BIC	HQIC	KS	p-value
			Data set: I				
TrMWED	(3.156; 4.025; 6.523)	61.63811	129.534	137.322	132.538	0.32151	0.9825
PQLD	(1.545; 1.152; 0.002)	61.86948	129.792	137.784	133.000	0.32788	0.9738
GIED	(0.831; 0.425; 1.648)	61.93259	129.864	137.910	133.126	0.32989	0.9712
EFWE	(0.082; 4.516; 1.324)	61.76434	129.528	137.574	132.790	0.32594	0.9753
EW	(0.345; 1.053; 0.564)	61.66522	129.330	137.376	132.592	0.32372	0.9779
UGIWD	(0.953; 1.526; 2.612)	61.78944	129.5788	137.625	132.841	0.32686	0.9745
TL-EE	(1.526; 0.859; 3.512)	61.82555	129.651	137.697	132.913	0.32727	0.9740
TGFrP	(1.632; 1.041; 3.415)	61.70123	129.402	137.448	132.665	0.32453	0.9768
TLLE	(0.452; 2.315; 4.023)	61.78225	129.564	137.610	132.827	0.32625	0.9749
			Data set: II				
TrMWED	(2.036; 3.225; 5.623)	88.11211	182.224	187.643	184.245	0.25111	0.97031
PQLD	(1.485; 1.315; 0.002)	88.14568	182.291	187.709	184.310	0.25848	0.96548
GIED	(0.643; 0.334; 1.326)	88.15629	182.312	187.731	184.332	0.25959	0.96329
EFWE	(0.004; 5.623; 0.425)	88.13567	182.271	187.689	184.290	0.25697	0.96767
EW	(0.804; 1.324; 0.084)	88.12533	182.250	187.669	184.270	0.25363	0.96893
UGIWD	(1.025; 0.832; 1.635)	88.12754	182.255	187.674	184.275	0.25464	0.96824
TL-EE	(2.631; 2.859; 0.845)	88.13476	182.269	187.689	184.289	0.25656	0.96786
TGFrP	(0.856; 4.326; 1.32)	88.11892	182.237	187.657	184.258	0.25282	0.96982
TLLE	(0.025; 1.145; 0.956)	88.13055	182.261	187.681	184.281	0.25525	0.96805
			Data set: III				
TrMWED	(1.956; 4.625; 4.985)	35.02612	74.052	83.044	78.846	0.05261	0.97651
PQLD	(1.325; 1.043; 0.002)	35.07655	76.153	83.145	78.947	0.05925	0.96785
GIED	(0.784; 0.556; 1.526)	35.08244	76.164	83.156	78.958	0.06157	0.96435
EFWE	(0.016; 2.574; 0.341)	35.06569	76131	83.122	78.924	0.05872	0.969954
EW	(0.136; 0.642; 0.023)	35.05623	76.112	83.104	78.906	0.05491	0.972126
UGIWD	(0.415; 1.025; 4.326)	35.45235	76.904	83.896	79.699	0.06232	0.96357
$TL-EE$	(2.301; 4.302; 1.023)	35.52135	77.042	84.034	79.837	0.06341	0.96125
TGFrP	(1.325; 4.253; 0.965)	35.05992	76.119	83.112	78.914	0.05682	0.97113
TLLE	(1.203; 2.635; 7.236)	35.06145	76.122	83.115	78.917	0.05758	0.97054

7 Conclusion

This paper introduces the truncated modified weighted exponential distribution (TrMWED), a novel extension of the modified weighted exponential distribution that incorporates an additional shape parameter and truncated support, thereby enhancing its flexibility. The statistical properties

of the TrMWED are rigorously derived, including moments, the moment-generating function, the quantile function, and order statistics. Parameter estimation is carried out using the maximum likelihood method, and the asymptotic properties of the estimators are investigated. Measures of uncertainty, namely Rényi and Tsallis entropies, are also obtained. The practical utility of the TrMWED is demonstrated through applications to three real-life datasets, where it consistently outperforms several competing distributions based on AIC and BIC criteria. These findings highlight the robustness and flexibility of the TrMWED, establishing it as a valuable model for analyzing lifetime and reliability data.

Acknowledgement: The authors would like to thanks Princess Nourah bint Abdulrahman University Researchers for Supporting number (PNURSP2025R226), Princess Nourah bint Abdulrahman University, Riyadh, Saudi Arabia.

Funding Statement: Princess Nourah bint Abdulrahman University Researchers Supporting Project number (PNURSP2025R226), Princess Nourah bint Abdulrahman University, Riyadh, Saudi Arabia.

Author Contributions: Conceptualization, Khaoula Aidi, Ghadah Alomani and Amer Ibrahim Al-Omari; Methodology, Amer Ibrahim Al-Omari, Ghadah Alomani and Khaoula Aidi; Software, Khaoula Aidi and Amer Ibrahim Al-Omari; Writing—review and editing, Ghadah Alomani, Khaoula Aidi and Amer Ibrahim Al-Omari; Investigation, Ghadah Alomani, Khaoula Aidi and Amer Ibrahim Al-Omari; Validation, Khaoula Aidi, Ghadah Alomani and Amer Ibrahim Al-Omari; Formal analysis, Khaoula Aidi and Amer Ibrahim Al-Omari; Writing—original draft, Ghadah Alomani, Khaoula Aidi and Amer Ibrahim Al-Omari; Data curation, Khaoula Aidi; Visualization, Khaoula Aidi and Amer Ibrahim Al-Omari; Funding acquisition, Ghadah Alomani. All authors reviewed the results and approved the final version of the manuscript.

Availability of Data and Materials: All the data sets used in this paper are available within the manuscript.

Ethics Approval: Not applicable.

Conflicts of Interest: The authors declare no conflicts of interest to report regarding the present study.

References

1. Zaninetti L. A right and left truncated gamma distribution with application to the stars. arXiv:1401.0287. 2014.
2. Singh S, Singh U, Sharma V. The truncated Lindley distribution: inference and application. J Stat Appl Probab. 2014;3:219–28.
3. Aguilar GA, Moala FA, Cordeiro GM. Zero-truncated Poisson exponentiated gamma distribution: application and estimation methods. J Stat Theory Pract. 2019;13:1–20. doi:10.1007/s42519-019-0059-2.
4. Shukla KK, Shanker R, Tiwari MK. Zero-truncated Poisson-Ishita distribution and its applications. J Sci Res. 2020;64:287–94. doi:10.37398/jsr.2020.640240.
5. Dey S, Altun E, Kumar D, Ghosh I. The reflected-shifted-truncated Lomax distribution: associated inference with applications. Ann Data Sci. 2021;10:805–28. doi:10.1007/s40745-021-00340-1.
6. Alotaibi N, Elbatal I, Almetwally EM, Alyami SA, Al-Moisheer AS, Elgarhy M. Truncated cauchy power weibull-G class of distributions: bayesian and non-bayesian inference modelling for COVID-19 and carbon fiber data. Mathematics. 2022;10:1565. doi:10.3390/math10091565.

7. Badr AM, Hassan T, El Din TS, Ali FA. Zero truncated Poisson-Pareto distribution: application and estimation methods. WSEAS Trans Math. 2023;22:132–8.
8. Abbas S, Farooq M, Darwish JA, Shahbaz SH, Shahbaz MQ. Truncated Weibull–exponential distribution: methods and applications. Sci Rep. 2023;13(1):20849. doi:10.1038/s41598-023-48288-x.
9. Hussein M, Rodrigues GM, Ortega EM, Vila R, Elsayed H. A new truncated Lindleygenerated family of distributions: properties, regression analysis, and applications. Entropy. 2023;25:1359. doi:10.3390/e25091359.
10. Teamah AEA, Elmenify HM. The doubly truncated generalized log-Lindley distribution. Appl Math. 2023;14:481–95. doi:10.4236/am.2023.147030.
11. Eledum H, El-Alosey A. Discrete Kumaraswamy Erlang-truncated exponential distribution with applications to count data. J Stat Appl Probab. 2023;12:725–39. doi:10.18576/jsap/120232.
12. Sen S, Alizadeh M, Aboraya M, Ali MM, Yousof HM, Ibrahim M. On truncated versions of Xgamma distribution: various estimation methods and statistical modelling. Stat Optim Inf Comput. 2024;12:943–61. doi:10.19139/soic-2310-5070-1660.
13. Zinodiny S, Nadarajah S, Nagar DK. A truncated matrix variate gamma distribution. Results Appl Math. 2024;22:100446. doi:10.1016/j.rinam.2024.100446.
14. Liu Y, Wang H, Xu Z, Mao J. Wind energy assessment considering a truncated distribution of probabilistic turbulence power spectral parameters. Renew Energy. 2024;223:119945. doi:10.1016/j.renene.2024.119945.
15. Abid S, Abdulrazak R. truncated Fréchet-G generator of distributions. Appl Math. 2017;3:51–66. doi:10.5923/j.am.20170703.03.
16. Bantan RA, Jamal F, Chesneau C, Elgarhy M. Truncated inverted Kumaraswamy generated family of distributions with applications. Entropy. 2019;21:1089. doi:10.3390/e21111089.
17. Al-Babtain AA, Elbatal I, Chesneau C, Jamal F. The transmuted Muth generated class of distributions with applications. Symmetry. 2020;12:1677. doi:10.3390/sym12101677.
18. Nik AS, Chesneau C, Bakouch HS, Asgharzadeh A. A new truncated (0, b)-F family of lifetime distributions with an extensive study to a submodel and reliability data. Afr Mat. 2023;34(1):3. doi:10.1007/s13370-022-01037-1.
19. Chesneau C, Kumar V, Khetan M, Arshad M. On a modified weighted exponential distribution with applications. Math Comput Appl. 2022;27(1):17. doi:10.3390/mca27010017.
20. Rényi A. On measures of information and entropy. In: Proceedings of the Fourth Berkeley Symposium on Mathematics, Statistics and Probability 1960. Oakland, CA, USA: University of California Press; 1961. p. 547–61.
21. Tsallis C. Possible generalization of Boltzmann-Gibbs statistics. J Stat Phys. 1988;52:479–87. doi:10.1007/bf01016429.
22. Swain JJ, Venkatraman S, Wilson JR. Least-squares estimation of distribution functions in Johnson's translation system. J Stat Comput Simul. 1988;29(4):271–97. doi:10.1080/00949658808811068.
23. Cheng R, Amin N. Estimating parameters in continuous univariate distributions with a shifted origin. J R Stat Soc Ser B. 1983;45:394–403. doi:10.1111/j.2517-6161.1983.tb01268.x.
24. Al-Mofleh H, Afify AZ, Ibrahim NA. A new extended two-parameter distribution: properties, estimation methods, and applications in medicine and geology. Mathematics. 2020;8:1578. doi:10.3390/math8091578.
25. Cheng R, Stephens M. A goodness-of-fit test using Moran's statistic with estimated parameters. Biometrika. 1989;76:385–92. doi:10.1093/biomet/76.2.385.
26. Dey S, Saha M, Maiti SS, Jun CH. Bootstrap confidence intervals of generalized process capability index Cpyk for Lindley and power Lindley distributions. Commun Stat Simul Comput. 2018;47(1):249–62. doi:10.1080/03610918.2017.1280166.
27. Boos D. Minimum Anderson-Darling estimation. Commun Stat Theory Methods. 1982;11:2747–74. doi:10.1080/03610928208828420.

28. Anderson TW, Darling DA. Asymptotic theory of certain "goodness of fit" criteria based on stochastic processes. Ann Math Stat. 1952;23:193–212. doi:10.1214/aoms/1177729437.
29. Rodrigues GC, Louzada F, Ramos PL. Poisson-exponential distribution: different methods of estimation. J Appl Stat. 2016;45(1):128–44. doi:10.1080/02664763.2016.1268571.
30. Akgül A. A novel method for a fractional derivative with non-local and non-singular kernel. Chaos Solitons Fractals. 2018;114:478–82.
31. Pal M, Ali MM, Woo J. Exponentiated Weibull distribution. Statistica. 2006;66:139–47.
32. El-Desouky BS, Mustafa A, Al-Garash S. The exponential flexible Weibull extension distribution. Open J Model Simul. 2017;16:83–97. doi:10.4236/ojmsi.2017.51007.
33. Alkarni SH. Power quasi Lindley distribution: properties and application. Asian J Math Comput Res. 2015;10:179–95.
34. Shala M, Merovci F. A new three-parameter inverse Rayleigh distribution: simulation and application to real data. Symmetry. 2024;16(5):634. doi:10.3390/sym16050634.
35. World Health Organization. WHO Coronavirus (COVID-19) Dashboard: cases [Internet]. 2025 [cited 2025 Oct 1]. Available from: https://data.who.int/dashboards/covid19/cases?n=c.
36. Kilai M, Waititu GA, Kibira WA, Alshanbari HM, El-Morshedy M. A new generalization of Gull Alpha power family of distributions with application to modeling COVID-19 mortality rates. Results Phys. 2022;36:105339. doi:10.1016/j.rinp.2022.105339.
37. Kalantan ZI, Binhimd SM, Salem HN, AL-Dayian GR, EL-Helbawy AA, Elaal MKA. Chen-Burr XII model as a competing risks model with applications to real-life data sets. Axioms. 2024;13:531. doi:10.3390/axioms13080531.
38. Aarset MV. How to identify a bathtub hazard rate. IEEE Trans Reliab. 1987;36:106–8. doi:10.1109/tr.1987.5222310.